Published by Institute of Physics Publishing for SISSA

Received: *December 7, 2006*
Accepted: *January 5, 2007*
Published: *February 6, 2007*

Holographic phase transitions at finite baryon density

Shinpei Kobayashi,[ab] **David Mateos,**[c] **Shunji Matsuura,**[ad] **Robert C. Myers**[abe] **and Rowan M. Thomson**[ab]

[a] *Perimeter Institute for Theoretical Physics, Waterloo, Ontario N2L 2Y5, Canada*
[b] *Department of Physics and Astronomy, University of Waterloo, Waterloo, Ontario, N2L 3G1, Canada*
[c] *Department of Physics, University of California, Santa Barbara, CA 93106-9530, U.S.A.*
[d] *Department of Physics, University of Tokyo, 7-3-1 Hongo, Bunkyoku, Tokyo, 113-0033, Japan*
[e] *Kavli Institute for Theoretical Physics, University of California, Santa Barbara, CA, 93106-4030, U.S.A.*
E-mail: skobayashi@perimeterinstitute.ca, dmateos@physics.ucsb.edu, smatsuura@perimeterinstitute.ca, rmyers@perimeterinstitute.ca, rthomson@perimeterinstitute.ca

Abstract: We use holographic techniques to study SU(N_c) super Yang-Mills theory coupled to $N_f \ll N_c$ flavours of fundamental matter at finite temperature and baryon density. We focus on four dimensions, for which the dual description consists of N_f D7-branes in the background of N_c black D3-branes, but our results apply in other dimensions as well. A non-zero chemical potential μ_b or baryon number density n_b is introduced via a nonvanishing worldvolume gauge field on the D7-branes. Ref. [1] identified a first order phase transition at zero density associated with 'melting' of the mesons. This extends to a line of phase transitions for small n_b, which terminates at a critical point at finite n_b. Investigation of the D7-branes' thermodynamics reveals that $(\partial\mu_b/\partial n_b)_T < 0$ in a small region of the phase diagram, indicating an instability. We comment on a possible new phase which may appear in this region.

Keywords: D-branes, Brane Dynamics in Gauge Theories.

JHEP02(2007)016

Contents

1. Introduction

In strongly coupled, large-N_c gauge theories with a gravity dual [2, 3], $N_f \ll N_c$ flavours of fundamental matter can be described by N_f D-brane probes [4] in the appropriate gravitational background. At sufficiently high temperatures, the latter contains a black hole [5]. Working with $N_f \ll N_c$ flavours ensures that the matter branes only make a small perturbation to this background. Then much of the physics can be studied in the probe approximation where the gravitational backreaction of these branes is neglected.[1]

This framework was recently used in [1, 7–9] to study the thermal properties of N_f flavours of fundamental quarks (and scalars) in SU(N_c) super Yang-Mills theories in diverse dimensions.[2] It was shown that a universal, first order phase transition occurs at some critical temperature T_{fun}. At low temperatures, the branes sit outside the black hole in what was dubbed a 'Minkowski' embedding (see figure 1), and stable meson bound states exist. In this phase the meson spectrum exhibits a mass gap and is discrete. Above some critical temperature T_{fun} the branes fall through the horizon in what were dubbed 'black hole' embeddings. In this phase the meson spectrum is gapless and continuous. This large-N_c, strong coupling phase transition is therefore associated with the melting of the mesons. In theories that undergo a confinement/deconfinement phase transition at some temperature $T_d < T_{fun}$, mesonic states thus remain bound in the deconfined phase for the range of temperatures $T_d < T < T_{fun}$.

This physics is in qualitative agreement with that of QCD, in which $s\bar{s}$ and $c\bar{c}$ states, for example, seem to survive the deconfinement phase transition at $T_d \simeq 175\,\mathrm{MeV}$ — see [7]

[1] The backreaction can not be ignored in calculating the effect of the fundamental matter on hydrodynamic transport coefficients such as the shear viscosity [6].

[2] Initial studies include [10, 11].

JHEP02(2007)016

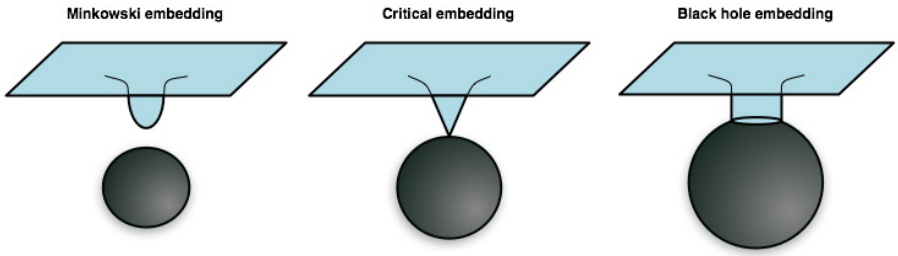

Figure 1: Various possible D7-brane embeddings in the black D3-brane geometry for zero baryon number density. The temperature increases from left to right. At finite $n_{\rm b}$, the Minkowski (and critical) embeddings are *not* allowed — see discussion in the text.

for a more detailed discussion. It is thus interesting to ask how this physics is modified at finite baryon density. In the presence of $N_{\rm f}$ flavours of equal mass, the gauge theory possesses a global $\mathrm{U}(N_{\rm f}) \simeq \mathrm{SU}(N_{\rm f}) \times \mathrm{U}(1)_{\rm q}$ symmetry. The $\mathrm{U}(1)_{\rm q}$ charge counts the net number of quarks, i.e., the number of baryons times $N_{\rm c}$ — see appendix A for details. In the gravity description, this global symmetry corresponds to the $\mathrm{U}(N_{\rm f})$ gauge symmetry on the worldvolume of the $N_{\rm f}$ D-brane probes. The conserved currents associated to the $\mathrm{U}(N_{\rm f})$ symmetry of the gauge theory are dual to the gauge fields on the D-branes. Thus, the introduction of a chemical potential $\mu_{\rm b}$ or a non-zero density $n_{\rm b}$ for the baryon number in the gauge theory corresponds to turning on the diagonal $\mathrm{U}(1) \subset \mathrm{U}(N_{\rm f})$ gauge field on the D-branes.[3]

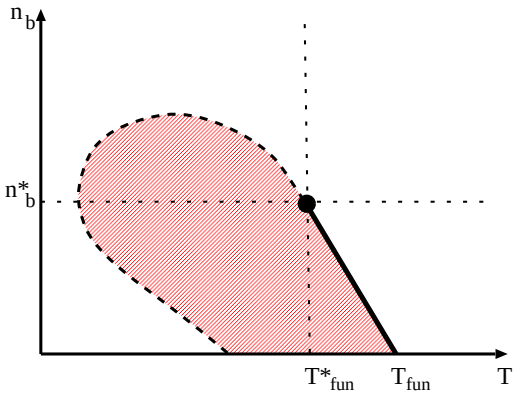

Figure 2: Phase diagram: Baryon number n_b versus temperature T. The line of first order phase transitions ends with a critical point at $(T^*_{\rm fun}, n^*_{\rm b})$. The phase which we study is intrinsically unstable in the shaded (red) region. This plot shows only a small portion of the full phase diagram near the critical point. The origin of the axes above corresponds to $(n_{\rm b}, T) = (0, 0.986\, T_{\rm fun})$.

In this paper we study the gauge theory at constant baryon number density $n_{\rm b}$. We find that, for any finite value of the baryon number density, the Minkowski embeddings, i.e., those embeddings where the probe brane closes off above the horizon, are physically inconsistent. Hence at finite $n_{\rm b}$, we focus our study on black hole embeddings. Despite this difference with the $n_{\rm b} = 0$ case, the first order phase transition found there continues to exist here for small enough a baryon number density. In this case, however, the transition is between two black hole embeddings. For a large enough baryon number density, there is no phase transition as a function of the temperature. The phase transition ceases to exist at a critical value $n^*_{\rm b}$. These results are summarised in figure 2. This phase diagram also shows a shaded region where the black hole embeddings are found to be thermodynamically unstable. While the boundary of this region shown in the

[3]This should not be confused with the chemical potential for R-charge (as considered in, e.g., [12, 13]) which is dual to internal angular momentum on the S^5 in the gravity description.

JHEP02(2007)016

diagram is qualitative, we have found that the unstable region has a limited extent to the left of the line of first order phase transitions. Hence the system must find a new stable phase, at least, in this small region — see section 3.

We focus on four-dimensional $\mathcal{N} = 4$ super Yang-Mills coupled to fundamental matter, whose dual description consists of $N_{\rm f}$ D7-branes in the background of $N_{\rm c}$ black D3-branes, but our results hold in other dimensions. Investigations of other holographic systems with a chemical potential have appeared previously in [14, 15]. An overview of the paper is as follows: In section 2, we solve for the embedding of the D7-branes in the black D3-brane geometry. Our discussion includes a brief review of the black hole background, the equations of motion determining the embedding, and a careful analysis of the required boundary conditions. In this section, we also discuss the effect of finite $n_{\rm b}$ on the critical solution and self-similar scaling found at $n_{\rm b} = 0$ [1, 7]. Finally we present the results of numerically solving for the embeddings at various values of the baryon number density. Section 3 examines the thermal properties of the D7-branes, including their stability or lack thereof. Section 4 concludes with a discussion of results. Appendix A presents some details of the holographic dictionary relating the worldvolume fields describing the D7-brane embeddings to their dual operators in the gauge theory.

2. Holographic framework

2.1 Black D3-branes

As first proposed in [2], $\mathcal{N} = 4$ super-Yang-Mills (SYM) with gauge group SU($N_{\rm c}$) is holographically dual to type IIB string theory on $AdS_5 \times S^5$ with $N_{\rm c}$ units of RR five-form flux. The dictionary relating the two sides of the duality equates $g_s = g^2_{\rm YM}/2\pi$ and $L^4/\ell_{\rm s}^4 = 2g^2_{\rm YM}N_{\rm c} \equiv 2\lambda$, where L is the AdS curvature scale — for a review, see [3]. In the limit of large $N_{\rm c}$ and large λ, the string side of the duality reduces to (weakly coupled) classical gravity. At a finite temperature, a black hole appears in the supergravity background [5]. Following [1, 7], the black hole metric may be written as[4]

$$ds^2 = \frac{1}{2}\left(\frac{\varrho}{L}\right)^2\left[-\frac{f^2}{\tilde{f}}dt^2 + \tilde{f}dx_3^2\right] + \frac{L^2}{\varrho^2}\left[d\varrho^2 + \varrho^2 d\Omega_5^2\right] , \tag{2.1}$$

where

$$f(\varrho) = 1 - \frac{u_0^4}{\varrho^4} , \quad \tilde{f}(\varrho) = 1 + \frac{u_0^4}{\varrho^4} . \tag{2.2}$$

The gauge theory temperature is then equivalent to the Hawking temperature of the black hole horizon, determined as usual by the surface gravity $T = \kappa/2\pi$. Alternatively, the latter temperature may be determined by demanding regularity of the Euclidean section obtained through the Wick rotation $t \to it_{\rm E}$. Then $t_{\rm E}$ must be periodically identified with a period β, where

$$\frac{1}{\beta} = T = \frac{u_0}{\pi L^2} . \tag{2.3}$$

[4]This metric is related to the standard presentation with the coordinate transformation $\varrho^2 = u^2 + \sqrt{u^4 - u_0^4}$.

This holographic framework allows the thermal behaviour of the strongly coupled gauge theory to be further studied with standard semiclassical gravity techniques [16]. In particular, the entropy density can be calculated as the geometric Hawking-Bekenstein entropy of the horizon [5, 17][5]

$$S = \frac{\mathcal{A}}{4G\,V_x} = \frac{\pi^6}{4G}\,\frac{L^8}{\beta^3} = \frac{\pi^2}{2}N_{\rm c}^2\,T^3\,, \tag{2.4}$$

where we have used $16\pi G = (2\pi)^7 \ell_s^8\, g_s^2$. The parametric dependence $S \propto N_{\rm c}^2$ reflects the fact that the gauge theory is deconfined. Remarkably, this strong coupling result differs from that calculated at weak coupling by merely a factor of 3/4 [17].

2.2 D7-brane embeddings

One feature of the $\mathcal{N} = 4$ SYM theory appearing in the duality above is that all of the fields transform in the adjoint representation of the SU($N_{\rm c}$) gauge group. Fields transforming in the fundamental representation can be included by introducing an additional set of D-branes on the string theory side of the duality. Following [4], we consider the decoupling limit of the intersection of $N_{\rm c}$ D3-branes and $N_{\rm f}$ D7-branes as described by the following array:

$$\begin{array}{lcccccccccc} & 0 & 1 & 2 & 3 & 4 & 5 & 6 & 7 & 8 & 9 \\ \text{D3:} & \times & \times & \times & \times & & & & & & \\ \text{D7:} & \times & \times & \times & \times & \times & \times & \times & \times & & \end{array} \tag{2.5}$$

The resulting dual gauge theory is $\mathcal{N} = 4$ super-Yang-Mills coupled to $N_{\rm f}$ $\mathcal{N} = 2$ fundamental hypermultiplets [4] at temperature T in $3+1$ dimensions. Assuming $N_{\rm f} \ll N_{\rm c}$, the decoupling limit leads to $N_{\rm f}$ probe D7-branes in the previous background (2.1), with the intersection being parametrised by the coordinates $\{t, x^i\}$. Since the D7-branes span the 4567-directions, it is useful to introduce spherical coordinates $\{r, \Omega_3\}$ in this space and polar coordinates $\{R, \phi\}$ in the 89-directions. Denoting by θ the angle between these two spaces we then have:

$$\varrho^2 = r^2 + R^2\,, \quad r = \varrho\sin\theta\,, \quad R = \varrho\cos\theta\,, \tag{2.6}$$

and

$$d\varrho^2 + \varrho^2 d\Omega_5^2 = d\varrho^2 + \varrho^2\left(d\theta^2 + \sin^2\theta\, d\Omega_3^2 + \cos^2\theta\, d\phi^2\right) \tag{2.7}$$

$$= dr^2 + r^2 d\Omega_3^2 + dR^2 + R^2 d\phi^2\,. \tag{2.8}$$

The analysis is simplified by taking $\chi = \cos\theta$ to describe the embedding of the D7-branes. Translational symmetry in the 0123-space and rotational symmetry in the 4567-directions motivate us to take $\chi = \chi(\varrho)$. The induced metric on the D7-branes is then:

$$ds^2 = \frac{1}{2}\left(\frac{\varrho}{L}\right)^2\left[-\frac{f^2}{\tilde{f}}dt^2 + \tilde{f}dx_3^2\right] + \frac{L^2}{\varrho^2}\left[\frac{1-\chi^2+\varrho^2(\partial_\varrho\chi)^2}{1-\chi^2}\right]d\varrho^2 + L^2(1-\chi^2)d\Omega_3^2\,. \tag{2.9}$$

[5] We divide out by the (formally infinite) three-dimensional volume V_x of the Minkowski space in which the gauge theory is formulated to yield the (finite) entropy density (2.4).

We also introduce a U(1) gauge field on the worldvolume of the D7-branes. As we discuss in detail in appendix A, in order to study the gauge theory at finite chemical potential or baryon number density, it suffices to turn on the time component of the gauge field, A_t. Again, symmetry considerations lead us to take the ansatz $A_t = A_t(\varrho)$. The action of the D7-branes then becomes:

$$I_{\rm D7} = -N_{\rm f} T_{\rm D7} \int d^8\sigma \frac{\varrho^3}{4} f\tilde{f}(1-\chi^2)\sqrt{1-\chi^2+\varrho^2(\partial_\varrho\chi)^2 - 2(2\pi\ell_{\rm s}^2)^2\frac{\tilde{f}}{f^2}(1-\chi^2)F_{\varrho t}^2}\,, \quad (2.10)$$

where $F_{\varrho t} = \partial_\varrho A_t$ is a radial electric field.

The equation of motion for A_t (Gauss' law) gives

$$\partial_\varrho \left[\frac{\varrho^3}{2}\frac{\tilde{f}^2}{f} \frac{(1-\chi^2)^2\partial_\varrho A_t}{\sqrt{1-\chi^2+\varrho^2(\partial_\varrho\chi)^2 - 2(2\pi\ell_{\rm s}^2)^2\frac{\tilde{f}}{f^2}(1-\chi^2)(\partial_\varrho A_t)^2}} \right] = 0\,. \quad (2.11)$$

In the limit that $\varrho \to \infty$, this equation reduces to $\partial_\varrho(\varrho^3\partial_\varrho A_t) \simeq 0$ and so the asymptotic solution approaches

$$A_t \simeq \mu - \frac{a}{\varrho^2} + \cdots\,. \quad (2.12)$$

The constants μ and a are (proportional to) the chemical potential for and the vacuum expectation value of the baryon number density, respectively (see appendix A). The equation of motion (2.11) clearly indicates that there is a constant of motion, which we write as

$$d \equiv N_{\rm f} T_{D7}(2\pi\ell_{\rm s}^2)^2\frac{\varrho^3}{2}\frac{\tilde{f}^2}{f} \frac{(1-\chi^2)^2\partial_\varrho A_t}{\sqrt{1-\chi^2+\varrho^2(\partial_\varrho\chi)^2 - 2(2\pi\ell_{\rm s}^2)^2\frac{\tilde{f}}{f^2}(1-\chi^2)(\partial_\varrho A_t)^2}}\,. \quad (2.13)$$

With this normalization, this constant is precisely the electric displacement, $d = \delta I_{\rm D7}/\delta F_{\varrho t}$. Taking the large-$\varrho$ limit of eq. (2.13) with the asymptotic form (2.12), we find:

$$d = N_{\rm f} T_{\rm D7}(2\pi\ell_{\rm s}^2)^2\, a. \quad (2.14)$$

Now one could proceed to derive the equation of motion for the D7-brane profile $\chi(\varrho)$ from the action (2.10) and then use eq. (2.13) to eliminate A_t in favor of the constant d. Instead, we first construct the Legendre transform of eq. (2.10) with respect to d to eliminate A_t directly at the level of the action. The result is:

$$\begin{aligned}\tilde{I}_{\rm D7} &= I_{\rm D7} - \int d^8\,\sigma F_{\varrho t}\frac{\delta I}{\delta F_{\varrho t}} \quad (2.15)\\ &= -N_{\rm f} T_{\rm D7}\int d^8\sigma\,\frac{\varrho^3}{4} f\tilde{f}(1-\chi^2)\sqrt{1-\chi^2+\varrho^2(\partial_\varrho\chi)^2}\left[1+\frac{8\,d^2}{(2\pi\ell_{\rm s}^2 N_{\rm f} T_{\rm D7})^2\varrho^6\tilde{f}^3(1-\chi^2)^3}\right]^{1/2}.\end{aligned}$$

The gauge field equations resulting from this Legendre transform are simply $\partial_\varrho d = \delta\tilde{I}_{\rm D7}/\delta A_t$ and $\partial_\varrho A_t = -\delta\tilde{I}_{\rm D7}/\delta d$. The first of these reproduces the fact that d is a fixed constant and we will return to the second one below.

Before deriving the equation of motion for the D7-brane profile $\chi(\varrho)$, it is convenient to introduce dimensionless quantities:

$$\rho = \frac{\varrho}{u_0}\,, \qquad \tilde{d} = \frac{d}{2\pi\ell_{\rm s}^2 u_0^3 N_{\rm f} T_{\rm D7}}\,. \tag{2.16}$$

The χ equation from eq. (2.15) can then be written as

$$\begin{aligned}\partial_\rho\left[\frac{\rho^5 f\tilde{f}(1-\chi^2)\dot{\chi}}{\sqrt{1-\chi^2+\rho^2\dot{\chi}^2}}\sqrt{1+\frac{8\tilde{d}^2}{\rho^6\tilde{f}^3(1-\chi^2)^3}}\right] &= -\frac{\rho^3 f\tilde{f}\chi}{\sqrt{1-\chi^2+\rho^2\dot{\chi}^2}}\sqrt{1+\frac{8\tilde{d}^2}{\rho^6\tilde{f}^3(1-\chi^2)^3}} \\ &\quad\times\left[3(1-\chi^2)+2\rho^2\dot{\chi}^2-24\tilde{d}^2\frac{1-\chi^2+\rho^2\dot{\chi}^2}{\rho^6\tilde{f}^3(1-\chi^2)^3+8\tilde{d}^2}\right],\end{aligned} \tag{2.17}$$

where the dot denotes derivatives with respect to ρ, i.e., $\dot{\chi} = \partial_\rho\chi$. With $\rho \to \infty$, this equation becomes at leading order: $\partial_\rho(\rho^5\dot{\chi}) \simeq -3\rho^3\,\chi$. Hence asymptotically the profile behaves as

$$\chi = \frac{m}{\rho} + \frac{c}{\rho^3} + \cdots\,, \tag{2.18}$$

where the dimensionless constants m and c are proportional to the quark mass and condensate, respectively [1, 7]. The precise relations are given in appendix A.

Returning to the gauge field, we begin by introducing a convenient dimensionless potential and chemical potential:

$$\tilde{A}_t = \frac{2\pi\ell_{\rm s}^2}{u_0}\,A_t\,, \quad \tilde{\mu} = \frac{2\pi\ell_{\rm s}^2}{u_0}\,\mu\,. \tag{2.19}$$

Then as described above, (2.15) yields the following equation

$$\partial_\rho\tilde{A}_t = 2\tilde{d}\frac{f^2\sqrt{1-\chi^2+\rho^2\dot{\chi}^2}}{\sqrt{\tilde{f}(1-\chi^2)[\rho^6\tilde{f}^3(1-\chi^2)^3+8\tilde{d}^2]}}\,. \tag{2.20}$$

Integrating yields the potential difference between two radii,

$$\tilde{A}_t(\rho) - \tilde{A}_t(\rho_0) = 2\tilde{d}\int_{\rho_0}^{\rho} d\rho\frac{f\sqrt{1-\chi^2+\rho^2\dot{\chi}^2}}{\sqrt{\tilde{f}(1-\chi^2)[\rho^6\tilde{f}^3(1-\chi^2)^3+8\tilde{d}^2]}}\,. \tag{2.21}$$

We will see below that all embeddings of interest extend down to the horizon at $\rho = 1$, so $\rho_0 = 1$ provides a convenient reference point. Further we set $\tilde{A}_t(\rho = 1) = 0$ by the following argument: The event horizon of the background (2.1) can be characterized as a Killing horizon, which implies that it contains the bifurcation surface where the Killing vector ∂_t vanishes [18]. If the potential $\tilde{A}$ as a one-form is to be well defined, then $\tilde{A}_t$ must vanish there. Hence we can use (2.21) to calculate the chemical potential, i.e., $\tilde{A}_t(\infty)$, as

$$\tilde{\mu} = 2\tilde{d}\int_1^{\infty} d\rho\,\frac{f\sqrt{1-\chi^2+\rho^2\dot{\chi}^2}}{\sqrt{\tilde{f}(1-\chi^2)[\rho^6\tilde{f}^3(1-\chi^2)^3+8\tilde{d}^2]}}\,. \tag{2.22}$$

JHEP02(2007)016

2.3 Near-horizon embeddings

An important role in [1, 7] was played by the analysis of the probe brane embeddings in the near-horizon region of the geometry (2.1). In this section we will see how this analysis is affected by the presence of the electric field on the D7-branes. In fact we will generalize the analysis to consider probe Dq-branes in a black Dp-brane background, along the lines of [1]. These calculations will lead to two main conclusions. The first one is that smooth Minkowski embeddings are unphysical for any non-zero baryon density. The second one is that we expect the first order phase transition found in [1, 7] to persist for small values of the baryon density, but to disappear for sufficiently large densities.

In order to focus on the near-horizon region, we set

$$\varrho = u_0 + \frac{L}{u_0} z\,, \quad \theta = \frac{y}{L}\,, \tag{2.23}$$

and expand the metric (2.1) to lowest order in z, y. This yields Rindler space together with some spectator directions which we omit since they will play no role in the following:

$$ds^2 = -(2\pi T)^2 z^2 dt^2 + dz^2 + dy^2 + y^2 d\Omega_n^2 + \cdots\,. \tag{2.24}$$

We recall that $T = u_0/\pi L^2$. In (2.24) we have introduced an integer n equal to the dimension of the internal sphere wrapped by the probe Dq-branes. For the D3/D7 system $n = 3$, but as stated above our analysis in this section will apply to more general Dp/Dq systems, for which possibly $n \neq 3$; for example, $n = 2$ for the D4/D6 system of [11]. The horizon is of course at $z = 0$. The coordinates z and y are the near-horizon analogues of the global coordinates R and r in (2.8), respectively.

In order to describe the embedding of the Dq-branes, we choose the static gauge for all their coordinates except the radial coordinate on the brane, which we denote as σ. The Dq-brane embedding may then be described parametrically as: $z = z(\sigma)$, $y = y(\sigma)$. We modify the analysis of [1] by adding a radial electric field $E \equiv \ell_s^2 \dot{A}_t/T$, where the dot denotes differentiation with respect to σ. For simplicity, in this section we will ignore the overall normalisation of the Dq-branes action and take $I_{\rm D7} \propto \int d\sigma \mathcal{L}$, where

$$\mathcal{L} = -y^n \sqrt{z^2(\dot{z}^2 + \dot{y}^2) - E^2}\,. \tag{2.25}$$

This action is homogeneous of degree $2 + n$ under the rescaling

$$z \to \alpha z\,, \quad y \to \alpha y\,, \quad E \to \alpha^2 E\,, \tag{2.26}$$

which means that the equations of motion will be invariant under such a transformation. Recall that as first described in [19], this scaling symmetry was a key ingredient for self-similarity of the brane embeddings in [1, 7]. However, in the present case with $E \neq 0$, the symmetry does not act within the family of embedding solutions with a fixed electric field (or rather fixed d — see eq. (2.28) below). Hence we can not expect to find exactly the same self-similar behaviour for branes supporting a fixed chemical potential or baryon density. However, we argue below that the embeddings should behave in approximately the same way at least where the gauge field is a small perturbation on the Dq-brane.

As in the previous subsection, it is convenient to work with the electric displacement

$$d = \frac{\partial \mathcal{L}}{\partial E} = \frac{y^n E}{\sqrt{z^2(\dot{z}^2 + \dot{y}^2) - E^2}}\,, \tag{2.27}$$

which is constant by virtue of Gauss' law. This is the near-horizon analogue of the quantity with the same name introduced in the previous subsection.[6] Note that under the scaling (2.26) d transforms as

$$d \to \alpha^n d\ . \tag{2.28}$$

Inverting the relation (2.27) above, one finds

$$E^2 = \frac{d^2 z^2(\dot{z}^2 + \dot{y}^2)}{d^2 + y^{2n}}\,. \tag{2.29}$$

It is also useful to note the relation

$$\sqrt{z^2(\dot{z}^2 + \dot{y}^2) - E^2} = y^n z \left[\frac{\dot{z}^2 + \dot{y}^2}{d^2 + y^{2n}}\right]^{1/2}\ . \tag{2.30}$$

To eliminate E in favour of d and obtain a functional for $y(\sigma)$ and $z(\sigma)$, we perform a Legendre transformation by defining

$$\tilde{\mathcal{L}} = \mathcal{L} - Ed = -z\sqrt{\dot{z}^2 + \dot{y}^2}\sqrt{d^2 + y^{2n}}\,, \tag{2.31}$$

in analogy with (2.15). It is easily verified that the equations of motion obtained from $\tilde{\mathcal{L}}$ are the same as those obtained by first varying $\mathcal{L}$ and then using eq. (2.29) to eliminate E.

We can conclude from eq. (2.29) that Minkowski embeddings which close off smoothly at the y-axis, such as those considered in [1, 7], are unphysical if $d \neq 0$. These embeddings are most appropriately described in the gauge $y = \sigma$, and they are characterised by the condition that the brane reaches $y = 0$ at some finite $z = z_0 > 0$. For the brane geometry to be smooth there, we must impose the boundary condition $\dot{z}(0) = 0$. Eq. (2.29) then yields $E^2 = z_0^2$ at $y = 0$. Now even though E remains finite, the tensor field $E dy \wedge dt$ is ill-defined at the origin and so one should conclude that these configurations are singular. This singularity is made clearer by considering the electric displacement d which also remains constant at the origin. However, one should note that as defined in eq. (2.27) d is actually a tensor density and so the norm of the associated tensor field is $\left|\frac{d}{\sqrt{-g}}\frac{\partial}{\partial y}\frac{\partial}{\partial t}\right|^2 \sim d^2/y^{2n}$, which clearly diverges at the origin. The physical reason why Minkowski embeddings are inconsistent is, of course, that the radial electric field lines have nowhere to end if the brane closes off above the horizon. This makes it clear that, although we have obtained this result in the near-horizon approximation, the same conclusion follows from an analysis in the full geometry (2.1).

For D-branes, an electric field on the worldvolume can also be associated with fundamental strings 'dissolved' into the the D7-brane [20] — see also the discussion around eq. (A.3). Hence the above statement that the electric field lines have nowhere to end

[6] Note, however, that they differ in their normalisation.

JHEP02(2007)016

can also be viewed as the fact that the strings have nowhere to end if the brane closes off. However, rather than simply viewing the Minkowski embeddings as unphysical, this point of view lends itself to the interpretation that these embeddings by themselves are incomplete. That is, one could imagine constructing a physical configuration by attaching a bundle of fundamental strings to the brane at $y = 0$ and letting these stretch down to the horizon. The strings resolve the singularity in the electric field since they act as point charges which are the source of this field. However, in such a configuration, the strings and the brane must satisfy a force balance equation at the point where they are connected. It is clear that if the brane closes off smoothly with $\dot{z}(0) = 0$, then they can not exert any vertical force in the z direction to balance the tension of the strings and so this can not be an equilibrium configuration. One might then consider 'cuspy' configurations which close off with a finite $\dot{z}(0)$ but still at some $z = z_0 > 0$. In this case, the branes exert a vertical force and so one must examine the configuration in more detail to determine if the two forces can precisely balance. This analysis requires a more careful treatment of the normalisation of the brane action and the fields than we have presented here. Hence we defer the detailed calculations to the next subsection where we will examine the D7-branes in more detail. However, let us state the conclusion here: no Minkowski embeddings can achieve an equilibrium for any (finite) value of $\dot{z}(0)$. Therefore we discard Minkowski embeddings for the rest of our analysis in the following.

Hence we now turn to consider black hole embeddings which intersect the horizon. Since these reach the horizon $z = 0$ at some $y = y_0$ they are conveniently described in the gauge $z = \sigma$. The appropriate boundary condition in this case is then $\dot{y}(0) = 0$, and the equation that follows from $\tilde{\mathcal{L}}$ is

$$(y^{2n} + d^2)\left[zy\ddot{y} + (1 + \dot{y}^2)y\dot{y}\right] - y^{2n}(1 + \dot{y}^2)nz = 0\,. \tag{2.32}$$

In view of this equation it is clear that we should expect two qualitatively different behaviours for solutions with $y_0^n \gg d$ and $y_0^n \ll d$. In the first case, it is easy to see that $y^n \gg d$ all along the solution, and so we effectively recover the equations of motion for $d = 0$ studied in [1, 7], and therefore oscillatory behaviour around a critical solution for large y:

$$y \simeq \sqrt{n}\, z + \xi\,, \quad \xi = \frac{T^{-1}}{(Tz)^{\frac{n}{2}}}\left[a\,\sin(\alpha \log Tz) + b\,\cos(\alpha \log Tz)\right]\,, \tag{2.33}$$

where a, b are determined by y_0. As shown in [1], this oscillatory behaviour eventually leads to the property that the quark condensate is multi-valued as a function of the quark mass, and hence to a first order phase transition (see figure 5 and the discussion in the next subsection). We thus expect a similar transition if $y_0^n \gg d$.

Incidentally, note that, unlike in the case $d = 0$, here the 'critical solution' $y = \sqrt{n}\, z$ is not an exact solution of eq. (2.32) but only an approximate solution for large y. In particular, there is no exact solution of the form $y \propto z$ that just touches the horizon except the $y = 0$ solution. Note also that for black hole embeddings eq. (2.29) gives $E \sim z$ as $z \to 0$, leading to a well defined tensor field at the horizon $z = 0$.

We now turn to the case $y_0^n \ll d$, for which the equation of motion (2.32) reduces to

$$z\ddot{y} + (1 + \dot{y}^2)\dot{y} \simeq 0\,, \tag{2.34}$$

whose exact solution is

$$\dot{y} = \frac{z_1}{\sqrt{z^2 - z_1^2}}\,, \tag{2.35}$$

$$y = y_0 + z_1 \log\left(z + \sqrt{z^2 - z_1^2}\right) c\,, \tag{2.36}$$

where y_0 and z_1 are integration constants. Recall that the boundary conditions should be $y(z = 0) = y_0$ and $\dot{y}(z = 0) = 0$. It is impossible to satisfy these conditions with the logarithm in eq. (2.36). It is also clearly seen in eq. (2.35) that the general solution is problematic (at $z = z_1$) unless $z_1 = 0$. Hence the only physical solution in this regime is precisely the constant solution: $y = y_0$.

Further, we note that the embedding starts very near the horizon with $y = y_0$ where $y_0^n \ll d$ and so we ask how it makes a transition to some more interesting profile of the full equation (2.32) far from the horizon. The point is that the term $ny^{2n}z$ will eventually grow large and require y to deviate from a constant. Quantitatively, one finds that the transition occurs for $z \sim y_0\,(d/y_0^n)$ where the leading solution has the form

$$y = y_0 + \frac{n}{4}\left(\frac{y_0^n}{d}\right)^2 \frac{z^2}{y_0} + \cdots\,. \tag{2.37}$$

Hence we see the $O(z^2)$ correction to the constant embedding is enormously suppressed in this regime $y_0^n \ll d$. Note that at $z \sim y_0\,(d/y_0^n)$, the second term is comparable to the first and so the Taylor series is breaking down. However, at this point, we still have $y^n \ll d$ and $\dot{y} \ll 1$. In summary, the solution in this regime is a long spike that emanates from the horizon almost vertically, resembling a bundle of strings.

The analysis above thus leads to the following physical picture. If d is small enough, then there is a set of embeddings in the near-horizon region for which $y_0^n \gg d$, whose physics is similar to that of the $d = 0$ case. In particular, we expect a first order phase transition to occur as a function of the temperature. As d increases, the region where the condition $y_0^n \gg d$ holds gets pushed outside the regime in which the near-horizon analysis is applicable, suggesting that the phase transition as a function of temperature should cease to exist for sufficiently large d. This is precisely what the phase diagram in figure 2 confirms. In contrast, the condition $y_0^n \ll d$ can always be met in the near-horizon region, indicating that solutions for which the part of the brane near the horizon behaves as a narrow cylinder of almost constant size, resembling a bundle of strings, exist for all values of d. This is also confirmed by our numerical analysis in the full geometry (as illustrated in figure 3), since such type of embeddings can always be realised, for any fixed d, by increasing the quark mass (or equivalently by decreasing the temperature). In the next subsection we analyse some properties of these embeddings more closely.

2.4 Strings from branes

The near-horizon analysis above revealed the existence of solutions for which the brane resembles a long narrow cylinder that emanates from the horizon. One's intuition is that this spike represents a bundle of strings stretching between the asymptotic brane and the

black hole. Examples in which fundamental strings attached to a D-brane are described as an electrically charged spike solution of the DBI action are well known in flat space [21], in AdS space [22] and in other brane backgrounds [23]. Here we would like to formalise this intuition by investigating the core region of our D7-brane embeddings in more detail. This analysis allows us to investigate the boundary conditions for the Minkowski-like embeddings in detail.

We begin by rewriting the Legendre-transformed action (2.15) as

$$\tilde{I}_{\rm D7} = -\frac{T_{\rm D7}}{\sqrt{2}} \int d^8\sigma \frac{f}{\tilde{f}^{1/2}} \sqrt{1+\frac{\varrho^2(\partial_\varrho\chi)^2}{1-\chi^2}} \left[\frac{d^2}{(2\pi\ell_{\rm s}^2 T_{\rm D7})^2} + \frac{N_{\rm f}^2}{8}\varrho^6\tilde{f}^3(1-\chi^2)^3\right]^{1/2} \tag{2.38}$$

Now recall that $\chi = \cos\theta$ — see eq. (2.7) — and consider the last factor in the integrand. If the embedding is very near the axis, i.e., $\chi \simeq 1$, then the second contribution in this factor can be neglected and eq. (2.38) becomes

$$\begin{aligned}\tilde{I}_{\rm D7} &\simeq -n_{\rm q}V_x\frac{1}{2\pi\ell_{\rm s}^2}\int dt\, d\varrho\, \frac{f}{(2\tilde{f})^{1/2}}\sqrt{1+\varrho^2(\partial_\varrho\theta)^2} \\ &= -n_{\rm q}V_x\frac{1}{2\pi\ell_{\rm s}^2}\int dt\, d\varrho\, \sqrt{-g_{tt}\,(g_{\varrho\varrho}+g_{\theta\theta}(\partial_\varrho\theta)^2)}\end{aligned} \tag{2.39}$$

where we have used the relation (A.4) between d and the density of strings $n_{\rm q}$. We recognize the result above as the Nambu-Goto action for a bundle of fundamental strings stretching in the ϱ direction but free to bend away from $\theta = 0$ on the S^5. It is interesting to note that the term that was dropped provides precisely the measure factor associated with the x^i and S^3 directions in the limit where the d term vanishes (or is small). In this sense then, the D7-brane forgets about its extent in those directions.

Let us consider the boundary conditions for the configurations which reach the axis $\theta = 0$ at some finite ϱ, i.e., for Minkowski-like embeddings. These embeddings would in general have a cusp if $\partial_\varrho\theta$ remains finite at $\theta = 0$ (a smooth embedding would correspond to $\partial_\varrho\theta \to \infty$). As discussed in the previous subsection, to produce a potentially physical configuration, we would attach a bundle fundamental strings to the tip of the brane (with precisely the density $n_{\rm q}$). However, to produce a consistent static configuration, there must be a balance between the forces exerted by these external strings and the brane along the ϱ-direction. The effective tension of the branes can be evaluated in many ways, but here we consider the calculation:

$$T_{\varrho\varrho} = \frac{2}{\sqrt{-g}}\frac{\delta\tilde{I}_{\rm D7}}{\delta g^{\varrho\varrho}} \simeq n_{\rm q}V_x\,\frac{1}{2\pi\ell_{\rm s}^2}\,\frac{g_{\varrho\varrho}}{\sqrt{1+g^{\varrho\varrho}g_{\theta\theta}(\partial_\varrho\theta)^2}}\,. \tag{2.40}$$

Now if we wish to calculate the effective tension for a bundle of strings smeared out of the x^i-directions with density $n_{\rm q}$, the same calculation would apply since eq. (2.39) is precisely the fundamental string action. However, these strings would lie vertically along the axis and so we would evaluate eq. (2.40) with $\partial_\varrho\theta = 0$. Hence for a cusp with any non-zero $\partial_\varrho\theta$, the effective tension (2.40) is less than that of the vertical strings. Hence none of these Minkowski-like embeddings can achieve an equilibrium with the attached strings for

JHEP02(2007)016

any finite value of $\partial_\varrho\theta$.[7] We might consider these configurations as the initial data in a dynamical context. Then, given the results above, we see that the strings will pull the brane down the axis to the horizon — a similar discussion appears in a different context in [24]. In any event, we will not consider any of these Minkowski-like embeddings in the remainder of our analysis.

Now let us consider the black hole embeddings that arise from eq. (2.39). In fact, the equations resulting from this action were studied as (a special case of) the string configurations describing Wilson loops in the AdS/CFT [25]. In general these solutions are loops which begin and end at large ϱ. Hence these are inappropriate in the present context.[8] In this context, at finite temperature, there is another class of string configurations, namely strings that fall straight into the horizon, which display the screening of the quark-antiquark potential. Using this experience, we conclude that the *only* solutions for eq. (2.39) which reach the horizon will be the constant configurations $\theta = \theta_0$. Hence, as we saw in the near horizon analysis, the black hole embeddings near the $\theta = 0$ axis are long narrow cylinders of constant (angular) cross-section.

One should ask how far out these constant profiles are valid as approximate solutions of the full equations derived from eq. (2.38). The approximation that allowed us to derive eq. (2.39) required $\tilde{d}^{1/3} \gg \rho \sin\theta$, assuming $\rho \gg 1$. Hence the constant solutions $\theta = \theta_0$ should remain approximate solutions out to $\rho_{\rm transition} \sim \tilde{d}^{1/3}/\theta_0$ for small $\theta_0 \ll 1$. Beyond this radius we expect the profile should expand out and approach an asymptotically flat brane. However, we can push this transition out to an arbitrarily large radius by taking $\theta_0 \to 0$. This again suggests that with $d \neq 0$, there are D7-brane embeddings which reach the horizon no matter how far the (asymptotic) brane is from the black hole. We will verify this result with numerical investigations of the full solutions for the action (2.38) in the next subsection.

Our analysis of the static D7-brane profiles near $\chi \sim 1$ have confirmed the idea that the embeddings develop a narrow spike that behaves like a bundle of strings stretching between the asymptotic brane and the black hole. It is interesting to extend this idea further by investigating the dynamical properties of these spikes. As a step in this direction, let us consider our framework with the more general ansatz: $\chi(\varrho, t)$ and $A_t(\varrho)$.[9] After a straightforward calculation the Legendre-transformed action becomes

$$\tilde{I}_{\rm D7} = -T_{\rm D7}\int d^8\sigma \frac{f}{(2\tilde{f})^{1/2}}\sqrt{1+\varrho^2(\partial_\varrho\theta)^2 - \frac{2L^4}{\varrho^2}\frac{\tilde{f}}{f^2}(\partial_t\theta)^2}\left[\frac{d^2}{(2\pi\ell_{\rm s}^2 T_{\rm D7})^2} + \frac{N_{\rm f}^2}{8}\varrho^6\tilde{f}^3\sin^6\theta\right]^{1/2}. \tag{2.41}$$

As above, we restrict our attention to the embeddings when they are very close to the axis $\theta \simeq 0$. In this regime, the second contribution in the last factor can be neglected and

[7] The same conclusion applies for the general Dq/Dp-brane configurations discussed in subsection 2.3.

[8] If we use only a portion of these solutions, i.e., the configuration is cut-off before reaching the loop's minimum ϱ, the profile describes the cuspy configurations discussed above.

[9] The symmetries of the problem ensure that this ansatz leads to a consistent solution.

JHEP02(2007)016

eq. (2.41) becomes

$$\tilde{I}_{\rm D7} \simeq -n_{\rm q} V_x \frac{1}{2\pi\ell_{\rm s}^2} \int dt\, d\varrho\, \frac{f}{(2\tilde{f})^{1/2}} \sqrt{1+\varrho^2(\partial_\varrho\theta)^2 - \frac{2L^4}{\varrho^2}\frac{\tilde{f}}{f^2}(\partial_t\theta)^2} \tag{2.42}$$

Once again we recognize this result as the Nambu-Goto action for a bundle of fundamental strings stretching in the ϱ-direction with dynamical fluctuations in the θ-direction. Hence we are beginning to see that not just the static properties of the spikes, such as the tension, but also their dynamical spectrum of perturbations matches that of a collection of strings; similar results have been seen for the dynamics of the BIon spikes on branes in asymptotically flat spacetime [26]. In this sense we see that, although no fundamental strings are initially manifest, the D7-brane spectrum still captures the presence of these strings. This is a satisfying result since these strings stretching between the horizon and the asymptotic D7-branes are dual to the quarks in the field theory, for which we are turning on chemical potential μ. It would be interesting to investigate these issues in more detail.

2.5 Numerical embeddings

We now return to the detailed analysis of the D7-brane embeddings in the black D3-brane background. In general, it is not feasible to solve analytically eq. (2.17), which determines the profile $\chi(\rho)$, so we resorted to numerics. We numerically integrated eq. (2.17), specifying boundary conditions on the horizon $\rho_{\rm min} = 1$: $\chi(1) = \chi_0$ for various $0 \le \chi_0 < 1$ and $\partial_\rho\chi|_{\rho=1} = 0$. In order to compute the constants m, c corresponding to each choice of boundary condition at the horizon, we fitted the solutions to the asymptotic form (2.18). Several representative D7-brane profiles are depicted in figure 3. In particular, we see explicitly here the formation of long narrow spikes reaching down to the horizon as χ_0 approaches 1 (or R approaches 1 on the horizon).

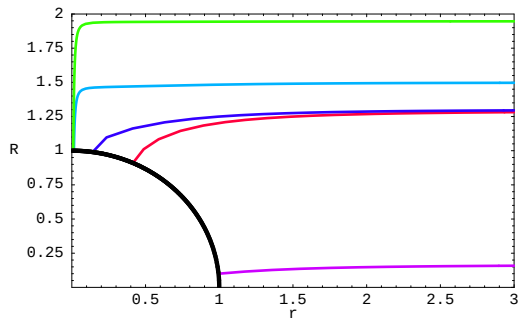

Figure 3: Profiles of various D7-brane embeddings in the D3-brane background for $\tilde{d} = 10^{-4}/4$. The black circle represents the horizon.

We can make the appearance of these spikes quantitative here by examining how varying boundary the condition χ_0 changes the quark mass m — recall that the latter is proportional to the distance which the branes reach along the vertical axis of figure 3. Figure 4 shows plots of m versus χ_0 for $\tilde{d} = 10^{-4}/4$ and $1/4$. Note that in both cases, as $\chi_0 \to 1$, the quark mass is diverging. Hence with $\tilde{d} \neq 0$, there are D7-brane embeddings which reach the horizon no matter how large the (asymptotic) separation between the brane and the black hole becomes. Since $m \propto M_{\rm q}/T$ as shown in eq. (A.2), $m \to \infty$ corresponds to $T \to 0$ for a fixed quark mass $M_{\rm q}$. Hence the previous result is equivalent to saying that the D7-branes intersect the horizon for all values of T when $d \neq 0$. Contrast this with the $\tilde{d} = 0$ case, where embeddings of the D7-branes which intersect the horizon (i.e., black hole embeddings) only

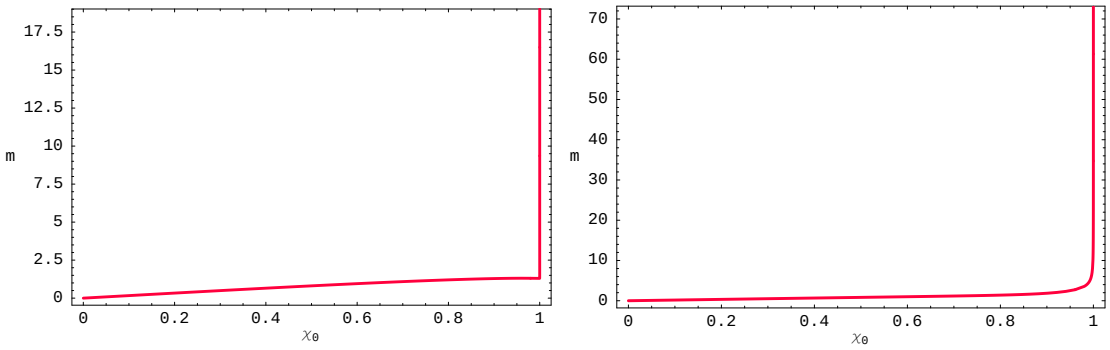

(a) (b)

Figure 4: Quark mass m versus boundary condition χ_0 on the horizon for (a) $\tilde{d} = 10^{-4}/4$ and (b) $\tilde{d} = 1/4$.

existed above some minimum temperature [1, 7]. At low temperatures the D7-branes were described by embeddings which smoothly closed off above the horizon (i.e., Minkowski embeddings). For nonzero chemical potential or nonzero baryon density, there are black hole embeddings corresponding to all temperatures in the gauge theory. For small temperatures, or large quark mass, most of the brane is very far away from the horizon with only a very thin long spike extending down to touch the horizon. Far from the black hole, this embedding would look very much like a Minkowski embedding in the low temperature phase of $\tilde{d} = 0$. It differs only by the narrow spike going down to touch the horizon.

Figures 5, 6 and 7 illustrate the dependence of the quark condensate c on the temperature T. Several such plots of c versus T with varying degrees of resolution are given in figure 5 for small values of the baryon density: $\tilde{d} = 0$, $10^{-6}/4$ and $10^{-4}/4$. In the first two plots, the differences between the curves is virtually indiscernable. In particular then, they all begin to show the spiralling behaviour that was characteristic of the self-similar scaling discovered for $\tilde{d} = 0$ [1, 7]. Of course, section 2.3 argued that these spirals should persist to a certain level at small $\tilde{d}$. Note that in the highest resolution plot (the last one in figure 5), one sees that for $\tilde{d} = 10^{-4}/4$ the small scale spirals have been eliminated. In any event, the plots in figure 5 explicitly demonstrate that, for small baryon density $\tilde{d}$, the black hole embeddings are mimicking the behaviour of both the black hole and Minkowski branches of the theory at $\tilde{d} = 0$. Hence certain features of the physics will be continuous between the theories with vanishing and non-vanishing baryon number density. In particular, the spiralling or rather the multi-valuedness of c indicates there will be a first order phase transition and so the 'melting' transition found in [1] persists to small values of the baryon density.

As $\tilde{d}$ is increased, the self-similar, spiralling behaviour becomes less and less pronounced and eventually c becomes a single-valued function of $T/\bar{M}$. To the best numerical accuracy that we could achieve, the critical value at which the phase transition disappears in $\tilde{d}^* = 0.00315$. Figure 6 shows the c in the vicinity of the transition around this critical value. For $\tilde{d} = 0.0031$, the curve shows a slight S-shape and so a small first order phase transition would still occur. For the critical value $\tilde{d}^* = 0.00315$, the curve is monotonic but with

JHEP02(2007)016

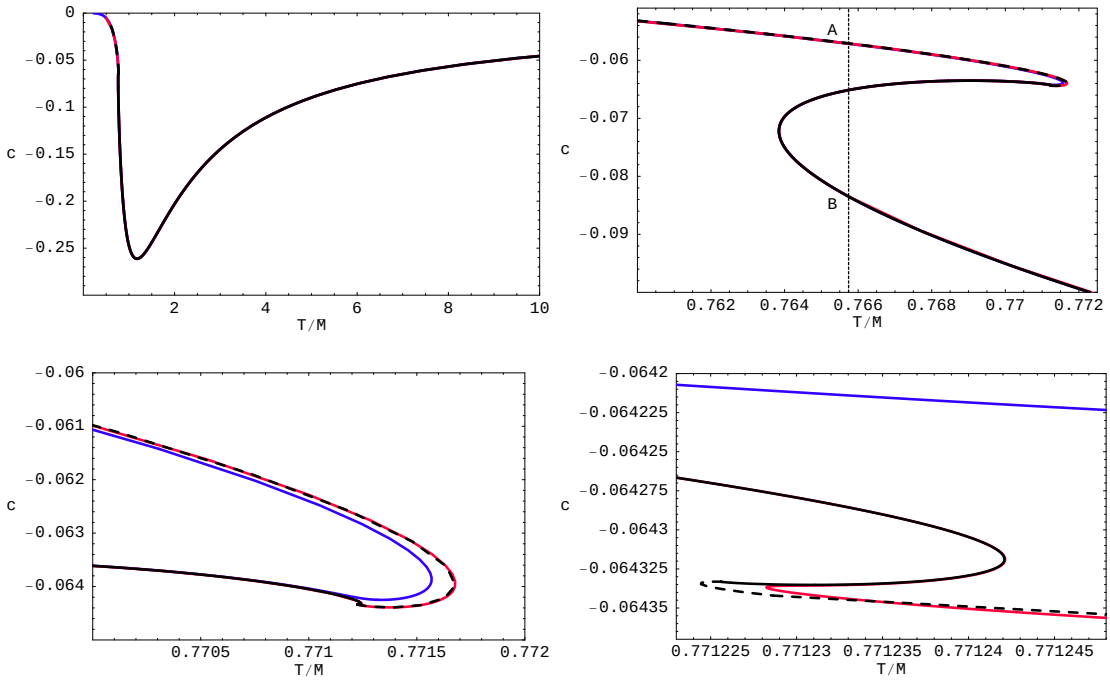

Figure 5: Quark condensate c versus temperature $T/\bar{M}$ for $\tilde{d} = 0$, $10^{-6}/4$ and $10^{-4}/4$ on the black, red and blue curves, respectively. At low resolution, these curves are all nearly identical and display a similar spiralling behaviour.

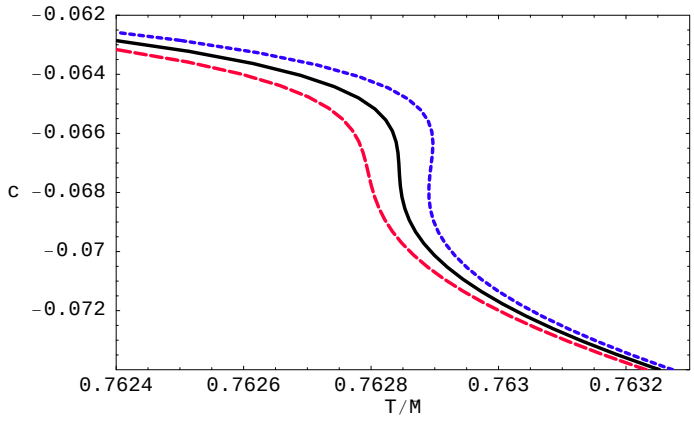

Figure 6: Quark condensate c versus temperature $T/\bar{M}$ near the critical point. The solid black curve corresponds to the critical baryon density $\tilde{d}^* = 0.00315$. The dashed curves above (blue) and below (red) correspond to $\tilde{d} = 0.0031$ and 0.0032, respectively.

a singular slope near the center. In this case, the phase transition would be reduced to second order. Finally for $\tilde{d} = 0.0032$, the curve is monotonic with a finite slope everywhere and so the phase transition has disappeared.

For completeness, we also show the behaviour of the quark condensate at much larger values of the baryon density in figure 7. Figure 7a corresponds to $\tilde{d} = 1/4$ where some

JHEP02(2007)016

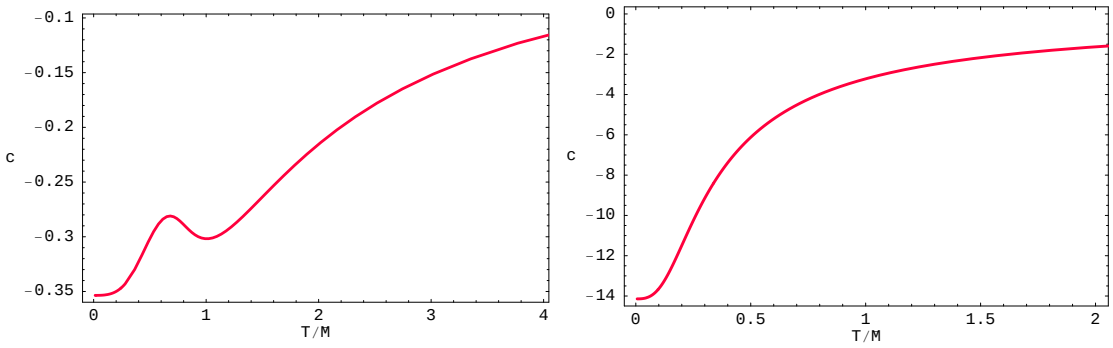

(a) (b)

Figure 7: Quark condensate c versus temperature $T/\bar{M}$ for (a) $\tilde{d} = 1/4$ and (b) $\tilde{d} = 10$.

interesting structure still persists around $T/\bar{M} \sim 1$, which was where c shows a minimum in figure 5 at smaller densities. Figure 7b corresponds to $\tilde{d} = 10$, where c has become a monotonically increasing (towards zero) function of T.

We integrated (2.22) numerically to solve for the chemical potential. Plots of $\tilde{\mu}$ versus temperature all show an apparent divergence as $T/\bar{M} \to 0$, as illustrated in figure 8a. However, this behaviour is misleading as we now explain. As discussed in the previous subsections, a common feature of the D7-brane embeddings at small temperatures is the long narrow spike close to the $\theta = 0$ axis. This spike dominates eq. (2.22) for small $T/\bar{M}$ and so the latter formula can be simplified to

$$\mu \simeq \frac{1}{\sqrt{2}2\pi\ell_s^2} \int_{u_0}^{u_0 m} d\varrho \, f/\tilde{f}^{1/2} \simeq M_{\rm q} \,, \tag{2.43}$$

where we have restored the dimensions of the chemical potential and the radial coordinate. Hence in this limit, the chemical potential is essentially given by the quark mass, as one might have expected. Hence the divergence in figure 8a arises simply because $\tilde{\mu} \propto \mu/T$, as shown in eq. (A.10). This spurious behaviour is eliminated by plotting $\mu/M_{\rm q} = \sqrt{2}\tilde{\mu}/m$, as shown in figure 8b. The latter plot exhibits the small temperature limit $\mu/M_{\rm q} \to 1$ for T approaching zero, as is implied by eq. (2.43). Note that if one calculates μ in the vicinity of the phase transition, it shows a multi-valuedness similar to that shown for the quark condensate above.

3. D7-brane thermodynamics: free energy, entropy and stability

We now wish to study the thermal properties of the fundamental hypermulitplets at finite baryon number. Our holographic framework translates this question into one of investigating the thermal contributions of the D7-branes on the gravity side. As usual, we use the standard technique [16] of Wick rotating the time direction. The Euclidean time circle of the black D3-brane background then becomes the thermal circle in a finite temperature path integral, and the leading contribution to the free energy is determined by evaluating the Euclidean action. As we are interested in the contributions of the fundamental matter,

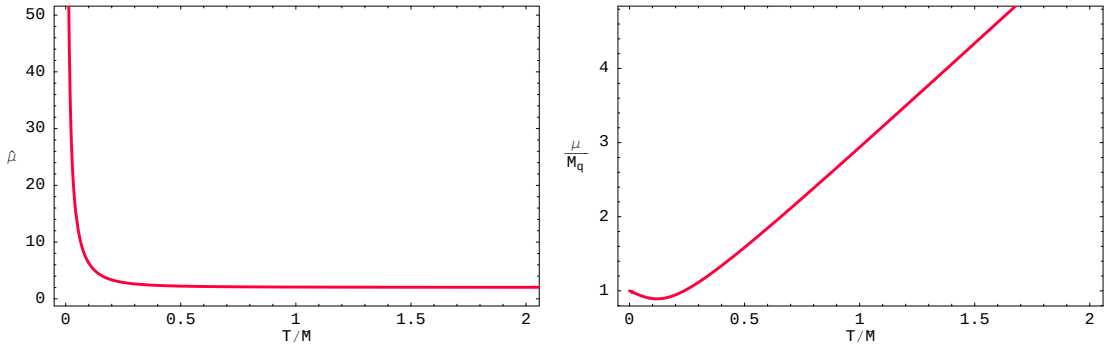

(a) (b)

Figure 8: Chemical potential for $\tilde{d} = 10$ versus temperature displayed as: (a) $\tilde{\mu}$ and (b) $\mu/M_{\rm q}$.

we only study the action of the D7-branes. Although evaluating the bulk brane action leads to a formally divergent result, the AdS/CFT correspondence provides a prescription to remove these divergences: One introduces a finite-radius UV cut-off and a set of boundary counterterms to renormalise the action [27]. This approach for the branes is completely analogous to the same calculations which are performed for the gravity background [28]. This holographic renormalisation of the D7-brane action was discussed in more detail in refs. [1, 7], which we follow closely in this section.

We begin by writing the Euclidean action for the D7-branes in terms of dimensionless quantities, introduced in section 2.2, as[10]

$$I_{\rm bulk} = \int d^8\sigma\, \mathcal{L}_{\rm E} = \mathcal{N} \int d^8\sigma\, \rho^3 f \tilde{f} (1-\chi^2) \sqrt{1-\chi^2+\rho^2\dot{\chi}^2 - \frac{2\tilde{f}}{f^2}(1-\chi^2)\dot{\tilde{A}}_t^2}\,, \tag{3.1}$$

where $\mathcal{N}$ is the normalisation constant introduced in [1, 7]:[11]

$$\mathcal{N} = \frac{2\pi^2 N_{\rm f} T_{\rm D7} u_0^4}{4T} = \frac{\lambda N_{\rm c} N_{\rm f} T^3}{32}\,. \tag{3.2}$$

The normalisation factor illustrates the fact that the leading contributions of the fundamental matter are proportional to $N_{\rm c}\, N_{\rm f}$, in accord with the large-$N_{\rm c}$ counting rules of the gauge theory. Note then that these contributions are subleading to those of the adjoint fields which scale as $N_{\rm c}^2$ — see, for example, the entropy density in eq. (2.4).

As commented above, this bulk action (3.1) contains large-ρ, UV divergences. Fortunately, however, these are the same as in the absence of the gauge field, and therefore no new counterterms are required beyond those derived in refs. [1, 7], which take the form

$$\frac{I_{\rm bound}}{\mathcal{N}} = -\frac{1}{4}\left({\rho_{\rm max}}^4 - 2m^2{\rho_{\rm max}}^2 + m^4 - 4mc\right)\,, \tag{3.3}$$

[10] For simplicity, we have left A_t untouched here rather than introducing a Wick rotated potential $A_{t_{\rm E}} = -i\,A_t$. As is well-known, such a Euclidean potential would have to be treated as an imaginary field in the present context because the chemical potential and particle density must remain real constants — see, e.g., [12].

[11] Note that this constant does not include the three-volume V_x along the gauge theory directions. Rather in this section we will divide out these factors everywhere and so all extensive quantities are actually densities per unit volume; for example, (3.1) is the Euclidean action density.

JHEP02(2007)016

where $\rho_{\rm max}$ is the UV cut-off. The regularised D7-brane action is then $I_{\rm E} = I_{\rm bulk} + I_{\rm bound}$. It can most simply be written as:

$$\frac{I_{\rm E}}{\mathcal{N}} = G(m) - \frac{1}{4}\left[({\rho_{\rm min}}^2 - m^2)^2 - 4mc\right] , \tag{3.4}$$

where $G(m)$ is the integral:

$$G(m) = \int_{\rho_{\rm min}}^{\rho_{\rm max}} d\rho \left(\rho^3 f \tilde{f}(1-\chi^2)\sqrt{1-\chi^2+\rho^2\dot{\chi}^2 - \frac{2\tilde{f}}{f^2}(1-\chi^2)\dot{\tilde{A}}_t^2} - \rho^3 + m^2\rho \right) . \tag{3.5}$$

The limit $\rho_{\rm max} \to \infty$ may now be taken, since this integral converges.

As usual, we wish to identify the action with a thermodynamic free energy. However, in the present case, there are various possibilities depending on the ensemble under consideration, i.e., the Gibbs free energy for the grand canonical ensemble with fixed μ and the Helmholtz free energy for the canonical ensemble with fixed $n_{\rm b}$. Now experience with similar calculations for charged black holes, e.g., [12], suggests that the Gibbs free energy is given by the Euclidean action while the Helmholtz free energy is associated with the Legendre transform of $I_{\rm E}$. Since we wish to work with fixed charge, we would want to work with the latter.

In the following, we confirm the above expectations. Using the equations of motion, the variation of the action reduces to a boundary term:

$$\delta I_{\rm E} = \left[\frac{\partial \mathcal{L}_{\rm E}}{\partial \dot{\chi}} \delta\chi + \frac{\partial \mathcal{L}_{\rm E}}{\partial \dot{\tilde{A}}_t} \delta\tilde{A}_t \right]_{\rho_{\rm min}}^{\rho_{\rm max}} . \tag{3.6}$$

Combining this with the variation of the boundary action $I_{\rm bound}$ (3.3) yields

$$\delta I_{\rm E} = -2\mathcal{N} c\, \delta m - \frac{n_{\rm q}}{T}\delta\mu \tag{3.7}$$

where $n_{\rm q}$ was defined in (A.4). Recalling that $m = \bar{M}/T$ we see that the natural thermodynamic variables of the Euclidean action are the temperature T and the chemical potential μ. Hence we must identify $I_{\rm E} = \beta W$, where $W(T,\mu)$ is the thermodynamic potential in the grand canonical ensemble, namely the Gibbs free energy.

Since we wish to work at fixed charge density, i.e., in the canonical ensemble,we perform a Legendre by defining

$$\tilde{I}_{\rm E} = I_{\rm E} + \frac{n_{\rm q}\,\mu}{T} , \tag{3.8}$$

which of course is a function of the temperature and the charge density:

$$\delta\tilde{I}_{\rm E} = -2\mathcal{N}\, c\, \delta m + \frac{\mu}{T}\,\delta n_{\rm q} . \tag{3.9}$$

We thus identify $\tilde{I}_{\rm E} = \beta F$ where $F(T, n_{\rm q})$ is the Helmholtz free energy.

The bulk part of $\tilde{I}_{\rm E}$ is of course the Euclidean analogue of (2.15):

$$\frac{\tilde{I}_{\rm bulk}}{\mathcal{N}} = \int d\rho\, \rho^3\, f\tilde{f}(1-\chi^2)\sqrt{1-\chi^2+\rho^2\dot{\chi}^2}\left[1 + \frac{8\tilde{d}^2}{\rho^6\tilde{f}^3(1-\chi^2)^3}\right]^{1/2} . \tag{3.10}$$

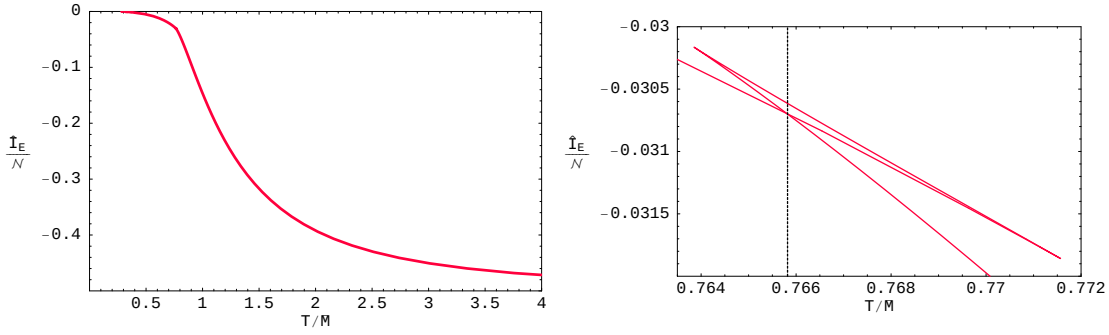

Figure 9: Legendre transform of the action, $\tilde{I}_{\rm D7}$, versus temperature for $\tilde{d} = 10^{-4}/4$. The phase transition temperature is denoted by the dotted vertical line in the second plot.

Since the divergences of this bulk action are the same as those of the $\tilde{d} = 0$ case, the analogous expression to eq. (3.4) is now

$$\frac{\tilde{I}_{\rm E}}{\mathcal{N}} = \widetilde{G}(m) - \frac{1}{4}\left[(m^2-1)^2 - 4mc\right] , \tag{3.11}$$

where $\widetilde{G}(m)$ is the integral:

$$\widetilde{G}(m) = \int_1^\infty d\rho \left[\rho^3 f \tilde{f}(1-\chi^2)\sqrt{1-\chi^2+\rho^2\dot{\chi}^2}\left(1+\frac{8\tilde{d}^2}{\rho^6\tilde{f}^3(1-\chi^2)^3}\right)^{1/2} - \rho^3 + m^2\rho\right] . \tag{3.12}$$

In both of these expressions, we have replaced $\rho_{\rm min} = 1$ since all of the embeddings which we consider terminate at the horizon.

We evaluated the free energy numerically for various $\tilde{d}$ and representative results are given in figures 9 and 11. The behaviour of the action versus temperature in figure 9 for $\tilde{d} = 10^{-4}/4$ is nearly identical to that for $\tilde{d} = 0$ — we refer the interested reader to compare with the plots presented in [1, 7]. The results for $\tilde{d} = 10^{-4}/4$ are typical for small values of $\tilde{d}$ with the classic 'swallow tail' shape. Of course, the crossing point of the two branches coming in from small and large T marks the temperature of the phase transition. By varying $\tilde{d}$, one can then map out the phase diagram shown above in figure 2. A more detailed diagram is shown here in figure 10. We see here that the first order phase transition occurs along a segment starting at $T_{\rm fun}/\bar{M} = .7658$ at $\tilde{d} = 0$ and ending at the critical point at $T^*_{\rm fun}/\bar{M} = .7629$ and $\tilde{d}^* = 0.00315$.

For completeness, we show some representative plots for large values of $\tilde{d}$ in figure 11, where there is no crossing and no phase transition. Note that these plots show an apparent divergence as $T \to 0$ but this is a spurious effect in analogy to the discussion of the plots for the chemical potential. This artifact is actually present in all of the free energy plots but the width becomes very narrow at small $\tilde{d}$.

We now turn to the entropy density. This can be obtained by differentiating the Helmholtz free energy density $F(T,d) = T\tilde{I}_{\rm E}$ with respect to T as

$$S = -\frac{\partial F}{\partial T} = -\pi L^2 \frac{\partial F}{\partial u_0} , \tag{3.13}$$

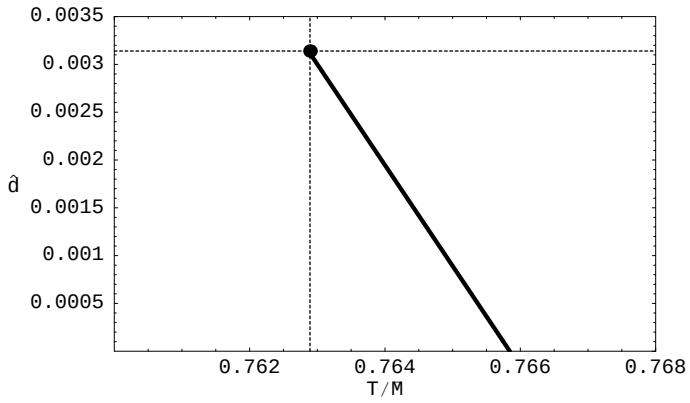

Figure 10: Phase diagram: Baryon density $\tilde{d}$ versus temperature $T/\bar{M}$.

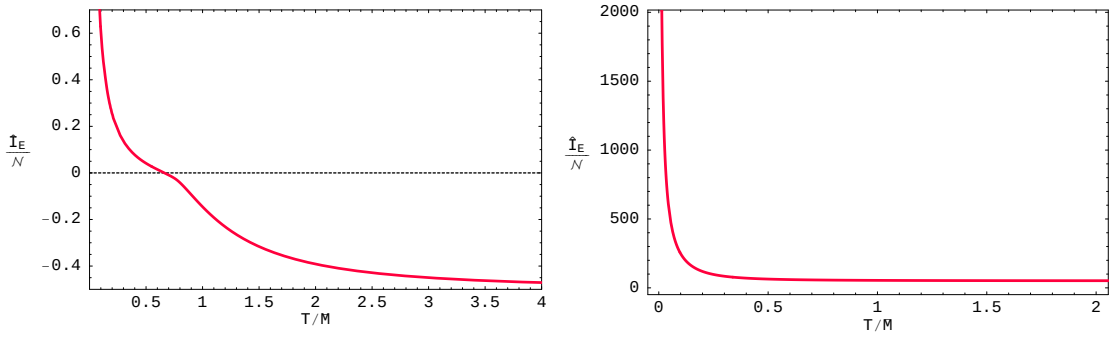

Figure 11: Legendre transform of the action, $\tilde{I}_{\rm D7}$, versus temperature for (a) $\tilde{d} = 10^{-1}/4$ and (b) $\tilde{d} = 10$. There is no phase transition for these values of $\tilde{d}$.

where we used the relation $u_0 = \pi L^2 T$. Following the calculations described in [7], one must carefully consider all of the implicit u_0 dependence in (3.11). The only new contribution comes here from the appearance of $\tilde{d}$ in (3.12) since from (2.16), we can see that

$$\frac{\partial \tilde{d}}{\partial u_0} = -\frac{3}{u_0}\tilde{d}\,. \tag{3.14}$$

Gathering all the contributions, the entropy can be expressed as

$$\frac{S}{\mathcal{N}} = -4\widetilde{G}(m) + 24\tilde{d}^2 H(m) + (m^2-1)^2 - 6mc. \tag{3.15}$$

Here we have defined the integral

$$H(m) = \int_1^\infty d\rho\, \frac{f\sqrt{1-\chi^2+\rho^2\dot{\chi}^2}}{\rho^3 \tilde{f}^2 (1-\chi^2)^2}\left[1 + \frac{8\tilde{d}^2}{\rho^6 \tilde{f}^3 (1-\chi^2)^3}\right]^{-1/2}. \tag{3.16}$$

Comparing this expression to eq. (2.22), we see that $H = \tilde{\mu}/2\tilde{d}$. Hence we may write the final result as

$$\frac{S}{\mathcal{N}} = -4\widetilde{G}(m) + 12\,\tilde{d}\tilde{\mu} + (m^2-1)^2 - 6mc\,. \tag{3.17}$$

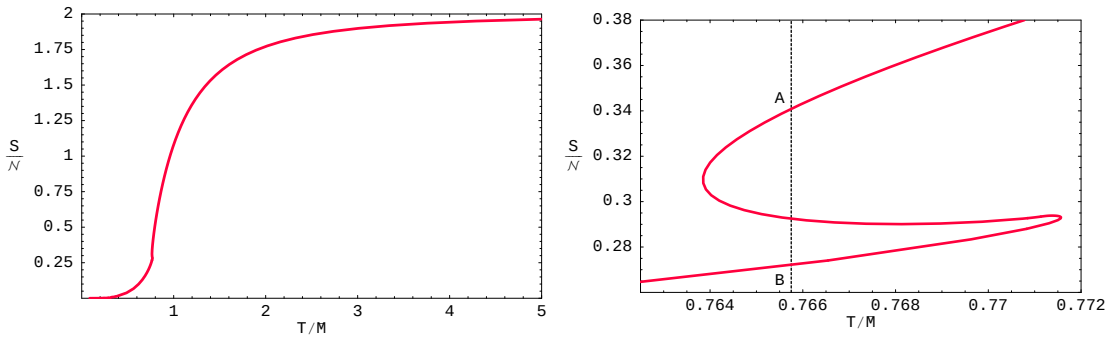

Figure 12: The entropy $S/\mathcal{N}$ versus temperature $T/\bar{M}$ for $\tilde{d} = 10^{-4}/4$. The position of the phase transition is marked by the dotted vertical line in the second figure.

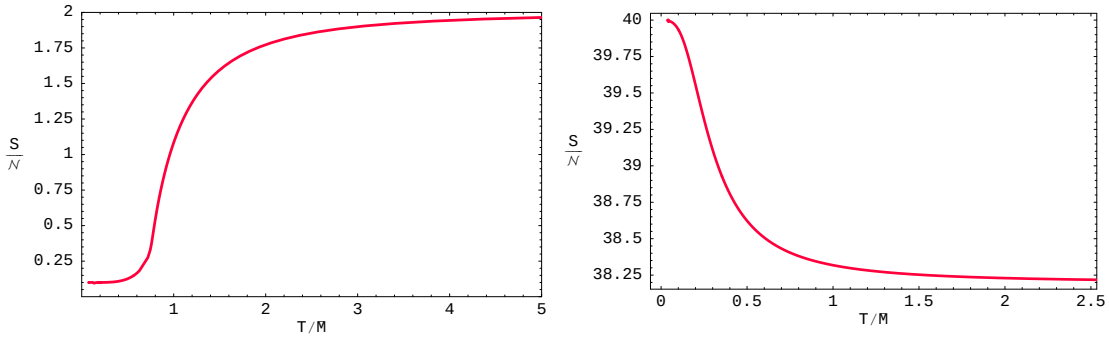

(a) (b)

Figure 13: The entropy $s/\mathcal{N}$ versus temperature $T/\bar{M}$ for (A) $\tilde{d} = 10^{-1}/4$ and (b) $\tilde{d} = 10$.

We evaluated the entropy numerically for various $\tilde{d}$ and some typical results are given in figures 12 and 13. The behaviour of the action versus temperature in figure 9 for $\tilde{d} = 10^{-4}/4$ is nearly identical to that for $\tilde{d} = 0$. In particular, near the phase transition point, the curve is multi-valued because there are several embeddings with the same values of $\tilde{d}$ and $T/\bar{M}$. We refer the interested reader to compare with the plots presented in [1, 7]. Figure 13 shows the behaviour of the entropy for larger values of $\tilde{d}$ beyond the critical point.

The thermodynamic identity $E = F + T\,S = T(\tilde{I}_{\rm E} + S)$ allows us to determine the contribution of the D7-brane to the energy density:

$$\frac{E}{\mathcal{N}T} = -3\widetilde{G}(m) + 12\,\tilde{d}\tilde{\mu} + \frac{3}{4}\left[(m^2-1)^2 - \frac{20}{3}mc\right] . \tag{3.18}$$

While we did calculate E for many values of $\tilde{d}$, we do not present any plots here as qualitatively their behaviour is similar to that in the plots of the entropy.

Finally, we turn to the thermodynamic stability of the system. There are various ways to write the requirements for the intrinsic stability of our fixed-charge ensemble. We investigated stability here with the conditions:

$$\frac{\partial S}{\partial T} > 0\,, \qquad \frac{\partial \mu}{\partial n} > 0\ . \tag{3.19}$$

The first one requires that the system be stable against fluctuations in energy and seems to be satisfied everywhere. The second constraint for electrical stability is more interesting, as we found that it was not satisfied for all $\tilde{d}$ and T. Our investigations of the region of instability remain preliminary, but figure 2 roughly illustrates the extent of the unstable zone as the shaded (red) region. In particular, the line of the phase transition seems to be part of the boundary of the unstable region between $T^*_{\rm fun}$ and $T_{\rm fun}$. This would indicate that the black hole embeddings do not correctly describe the true ground state in this small region and in particular, just below the phase transition. We hope to return to this matter in the future. We comment more on the implications of the instability in the discussion section below.

4. Discussion

Ref. [1] identified a universal, first order thermal phase transition in holographic Dp/Dq systems. This was characterised by a jump of the Dq-branes between a Minkowski embedding and a black hole embedding in the background of the black Dp-branes. In the gauge theory this transition is associated to the melting of the mesons.

Here we have shown that Minkowski embeddings become inconsistent at any finite baryon (or equivalently, quark) number density. The physical reason is that a non-zero density which is dual to a worldvolume electric field translates into a finite number of strings being dissolved into the Dq-branes. Hence the brane is not allowed to close off smoothly as the strings cannot simply terminate. We considered the possibility of Minkowski-like embeddings where the branes close off above the horizon and external fundamental strings are attached at this point and extend down to the horizon. However, examining the forces between the cusp in the brane embedding and the external strings, one finds that no equilibrium configuration is possible. Rather the strings would pull the tip of the brane down to meet the horizon. We note here though that this is not the only possibility for a Minkowski-like embedding. One must simply attach a source for the strings and one obvious alternative for such source is the baryon vertex [22]. In a Dp-brane background, the baryon vertex consists of a D(8–p)-brane wrapping the internal S^{8-p}. Hence it may be that there is a family of Minkowski-like embeddings, where a gas of baryons absorbs the strings dissolved on the probe branes. It would be interesting to investigate this possibility further.

On the other hand, we did find that with any non-zero baryon density $n_{\rm b}$, black hole embeddings where the Dq-branes intersect the horizon exist for all values of the temperature. In contrast, such embeddings do not exist below a certain temperature for $n_{\rm b} = 0$ and the system must be described by a Minkowski embedding beyond this point. In any event, we focused here on studying the behaviour of the black hole embeddings at finite $n_{\rm b}$ in the specific example of the D3/D7 system. Our results indicate that the physics is essentially continuous around $n_{\rm b} = 0$. The reason is that black hole embeddings with very small $n_{\rm b}$ mimic the behaviour of both $n_{\rm b} = 0$ Minkowski embeddings and $n_{\rm b} = 0$ black hole embeddings. Moreover, the near-horizon analysis strongly suggested that the universal phase transition found in [1] should persist for sufficiently small baryon densities,

JHEP02(2007)016

but that it should cease to exist above some critical value $n_b = n_b^*$. This was confirmed by our detailed numerical analysis for the D3/D7 system. We emphasize though that the transition at small baryon density occurs between two black hole embeddings.

At zero baryon number density, the spectrum on Minkowski embeddings consists of a gapped, discrete set of stable mesons (in the large-N_c, strong coupling limit), together with stable, massive, free constituent quarks [1, 7]. Instead, mesons on black hole embeddings have melted and and the spectrum is continuous and gapless. In fact, little evidence of the previously stable states remains in this continuous spectrum [29]. In addition, constituent quarks are massless. In the presence of a non-zero baryon density, all embeddings are of black hole type and hence no strictly stable mesons exist. Note, however, that the decay width is very small if the quark mass is very large, or if the meson is very heavy. Indeed, the decay width of a meson is proportional to the support of its wave function on the near-axis region where the spike attaches to the branes. This region becomes small as the quark mass increases. Alternatively, the peak of the meson wave function occurs further and further away from the axis as the meson mass increases — which, for fixed quark mass, can be achieved by, for example, increasing the meson radial quantum number. We plan to study these issues in more detail elsewhere.

Similarly, it may seem that the free constituent quarks represent a puzzle in this framework. Recall that the dual gauge theory is deconfined and so free quarks should play a role, in particular since we introduce a chemical potential. The analysis at $n_b = 0$ suggests that at least at low temperatures a constituent quark is dual to a string extending from the horizon to the brane (at large radius). However, at finite n_b, our embeddings are all of the black hole type and so if we attach such a string to the brane, it will quickly slip away behind the horizon. Hence the puzzle is: How do the D7-branes capture the physics of a gas of constituent quarks at low temperatures when there are no stable excitations corresponding to macroscopic strings?

Of course, the resolution of this puzzle is provided by the analysis in subsection 2.4. The near-horizon analysis of the Dp/Dq system suggested that, for any value of the baryon density, there should exist Dq-brane embeddings which resemble closely Minkowski embeddings everywhere except for a long thin spike stretching all the way down to the black Dp-branes horizon. This was confirmed for the D3/D7 case by our numerical results, which demonstrate that such embeddings correspond to large quark masses (or low temperatures). Further, we showed that not only do these spikes match the tension of a bundle of fundamental strings, but also their dynamics. Hence these spikes provide a brane realisation of the desired gas of constituent quarks. Since the fields describing the D7-branes are dual to meson operators (i.e., operators with $n_q = 0$) in the gauge theory, we may say that, in a very precise sense, quarks are being built out of mesons here, in the limit of large quark masses.

In considering the discussion above, one must remember that part of our phase diagram 2 corresponds to unstable embeddings. In particular, the line of the phase transition seems to be part of the boundary of the unstable region. This would indicate that the black hole embeddings do not correctly describe the true ground state of the phase immediately below the phase transition. Hence while one should not doubt the existence

JHEP02(2007)016

of a phase transition, the precise location of the transition can be called into question. Recall however, that for small $\tilde{d} \neq 0$ the behaviour of the black hole embeddings matched everywhere the known behaviour of the system with $\tilde{d} = 0$ very closely, as illustrated in figure 5. Hence we expect that the true line of phase transitions must be very close to that indicated in figure 10 for small $\tilde{d}$ but it may deviate to the right at larger values of $\tilde{d}$. We also reiterate that we are still refining our results on the boundary of the unstable region and that figure 2 only gives a qualitative representation beyond $T^*_{\rm fun}$. It may also be that the region below the phase transition line very close to $T_{\rm fun}$ is stable.

The instability arises in the region where

$$\left(\frac{\partial \mu}{\partial n_{\rm b}}\right)_T = \left(\frac{\partial^2 F}{\partial n_{\rm b}^2}\right)_T < 0\,. \tag{4.1}$$

It would of course be interesting to identify what the stable ground state is in this region. One indication comes from the nature of the instability itself. In the region where (4.1) holds the free energy F is a concave function of the baryon density, which means that the system can lower its free energy by separating into two phases with densities $n_{\rm b}^1 < n_{\rm b} < n_{\rm b}^2$ such that

$$\gamma n_{\rm b}^1 + (1-\gamma) n_{\rm b}^2 = n_{\rm b}\,, \quad \gamma F(n_{\rm b}^1) + (1-\gamma) F(n_{\rm b}^2) < F(n_{\rm b})\,. \tag{4.2}$$

One way in which this would be realised in the gravity description would be that it becomes thermodynamically favourable for the $N_{\rm f}$ D-brane probes to distribute the $\mathrm{U}(1)_q$ charge unequally among constituent branes, presumably through some mechanism involving the non-Abelian nature of their dynamics. This would imply that the flavour symmetry is spontaneously broken in the infrared. Alternatively, such a separation in different-$n_{\rm b}$ phases may be realised by going to a spatially inhomogeneous phase where $n_{\rm b}$ varies from point to point. Either of these speculative possibilities would imply that the flavour symmetry is spontaneously broken in the infrared. The Minkowski-like embeddings carrying a gas of baryons may play a role in this regime. We would also note that at this point, it is not clear whether or not other phases or embeddings will also play a role beyond the region of instability. In particular, we suspect that a new phase may appear at very low temperatures.

In this paper we have concentrated on the phase structure of gauge theories at constant temperature and charge density, namely on their description in the canonical ensemble. It will be interesting to consider the phase structure of these theories in the grand canonical ensemble, i.e., as a function of the temperature and the chemical potential. This should be particularly interesting in terms of a potential comparison with the phase structure of QCD. However, it is important to keep in mind that much of the interesting physics in QCD at finite density — see, e.g., [30] — is associated to the fact that baryon number in QCD is only carried by fermionic fields (quarks). This leads to the existence of a Fermi surface at finite chemical potential. In gauge theories dual to Dp/Dq systems as those considered here, baryon number is also carried by scalar fields, and so the physics at finite chemical potential is likely to be very different. In particular, a chemical potential for charged scalars acts effectively as a negative mass squared. In the case of free massless scalars this

JHEP02(2007)016

leads to an instability. The theories considered here, however, contain interaction, quartic terms in the fundamental scalars, and so the chemical potential will presumably lead to condensation of the scalars if these are sufficiently light.

Acknowledgments

It is a pleasure to thank S. Hartnoll, T. Hiramatsu, Y. Hisamatsu, G. Horowitz, A. Karch, P. Kumar, A. Naqvi, Y. Sendouda, D.T. Son and A.O. Starinets for useful conversations. Research at the Perimeter Institute is supported in part by funds from NSERC of Canada and MEDT of Ontario. We also acknowledge support from NSF grant PHY-0244764 (DM), NSERC Discovery grant (RCM), JSPS Postdoctoral Fellowship for Research Abroad (SK), JSPS Research Fellowships for Young Scientists (SM) and NSERC Canada Graduate Scholarship (RMT). Research at the KITP was supported in part by the NSF under Grant No. PHY99-07949.

While this paper was being prepared, we became aware of [31] which overlaps considerably with the present work. We thank Sang-Jin Sin for informing us of their project before publication. Unfortunately we find no evidence of two phase transitions as reported in [31]. We believe their result is spurious, arising from including unphysical Minkowski embeddings in their analysis.

A. Holographic dictionary

As described in section 2, the D7-brane embeddings are characterized by two nontrivial functions, $\chi(\rho)$ and $A_t(\rho)$. Further, as usual in AdS/CFT-like dualities, the asymptotic behaviour of these fields has a direct translation in terms of operators in the dual gauge theory [3]. In particular, considering the asymptotic behaviour in eqs. (2.12) and (2.18), the leading term corresponds to the non-normalizable mode and its amplitude indicates the coefficient with which the operator is added to the microscopic Lagrangian of the field theory. Similarly, the subleading term is the normalizable mode and its amplitude is proportional to the vacuum expectation value of the operator. In the present case, since we are discussing worldvolume fields, the corresponding operators involve fundamental hypermultiplet fields.

Let us remind the reader that a hypermultiplet consists of two Weyl fermions $\psi, \tilde{\psi}$ and two complex scalars $q, \tilde{q}$ – the quarks of our theory. These are naturally organized so that ψ and q transform in the fundamental of the $\mathrm{SU}(N_\mathrm{c})$ gauge group, while $\tilde{\psi}$ and $\tilde{q}$ transform in the antifundamental. Further, with N_f flavours (of equal mass), the hypermultiplets transform under a global $\mathrm{U}(N_\mathrm{f}) \simeq \mathrm{SU}(N_\mathrm{f}) \times \mathrm{U}(1)_\mathrm{q}$ symmetry. The charges of the fields under the diagonal $\mathrm{U}(1)_\mathrm{q}$ are $+1$ for ψ and q and -1 for $\tilde{\psi}$ and $\tilde{q}$. Hence the $\mathrm{U}(1)_\mathrm{q}$ charge naturally counts the net number of quarks in a given state. As the colour group is $\mathrm{SU}(N_\mathrm{c})$, baryons are composed of N_c quarks and so we would divide by N_c for the number of baryons.

Now the operators dual to $\chi(\rho)$ and $A_t(\rho)$ can be determined by considering the interactions of the open strings on the D3/D7 array (2.5) before the decoupling limit [32], in

analogy with the closed strings. Such an exercise leads to the following two operators:

$$\begin{aligned} A_t \leftrightarrow \mathcal{O}_{\rm q} &= \psi^\dagger\psi + \tilde\psi\tilde\psi^\dagger + i(q^\dagger\mathcal{D}_t q - (\mathcal{D}_t q)^\dagger q) + i(\tilde q\,(\mathcal{D}_t\tilde q)^\dagger - \mathcal{D}_t\tilde q\,\tilde q^\dagger)\,. \\ \chi \leftrightarrow \mathcal{O}_{\rm m} &= i\tilde\psi\psi + \tilde q(M_q + \sqrt{2}\Phi)\tilde q^\dagger + q^\dagger(M_q + \sqrt{2}\Phi)q + h.c.\,, \end{aligned} \tag{A.1}$$

Recall that the global flavour symmetry discussed above is the $\mathrm{U}(N_{\rm f})$ gauge symmetry of the $N_{\rm f}$ D7-brane worldvolume. Hence $\mathcal{O}_{\rm q}$ is simply the quark charge density, i.e., the time component of the conserved $\mathrm{U}(1)_{\rm q}$ current gauged by A_μ on the D7-brane. Note that the $\mathcal{D}_t$ indicate covariant time derivatives in the $SU(N_{\rm c})$ gauge theory. The operator $\mathcal{O}_{\rm m}$ is the variation of the mass term in the microscopic Lagrangian, i.e. $\mathcal{O}_{\rm m} = -\partial_{M_{\rm q}}\mathcal{L}$. Note that Φ, one of the adjoint scalars in the $\mathcal{N}=4$ supermultiplet, as well as M_q, appear in the scalar terms here after solving for the auxiliary field constraints within the full coupled theory. As a check, one can observe that both of these operators have conformal dimension[12] $\Delta = 3$, which matches the standard prescription for the asymptotic powers appearing in eqs. (2.12) and (2.18).

Now we can make the dictionary between the asymptotic coefficients and the dual gauge theory parameters precise by realizing that the hypermultiplet states are the ground states of the 3-7 and 7-3 strings. Hence in the decoupling limit, these become precisely strings stretching between the D7-brane and the horizon of the D3-brane. For example, the quark mass is trivially derived for the brane array (2.5) in asymptotically flat space. As this brane configuration is supersymmetric at $T=0$, this mass persists in the decoupling limit, where it is again the energy of a string stretching between the D3- and D7-branes. This gives a relation between $M_{\rm q}$ and the parameter m appearing in eq. (2.18). Further this relation is inherited by the theory at finite temperature, since setting $T \neq 0$ does not alter the asymptotic properties that determine the gauge theory parameters.[13] Using this result, we can formulate a variational argument [11] to relate the second coefficient in the asymptotic expanision of χ to the field theory condensate $\langle i(\tilde\psi\psi - \psi^\dagger\tilde\psi^\dagger)\rangle$.[14] As the details of this analysis can be found elsewhere [11, 7],[15] we simply present the results:

$$\begin{aligned} M_{\rm q} &= \tfrac{u_0}{2^{3/2}\pi\ell_{\rm s}^2}\,m & \langle\tilde\psi\psi\rangle &= -2^{3/2}\pi^3\ell_{\rm s}^2 N_{\rm f} T_{\rm D7} u_0^3\,c \\ &= \tfrac{1}{2}\sqrt{\lambda}\,T\,m & &= -\frac{1}{8}\sqrt{\lambda}\,N_{\rm f}\,N_{\rm c} T^3\,c\,. \end{aligned} \tag{A.2}$$

Given this result, we note that various figures were plotted in terms of $T/\bar M \equiv 1/m$ and hence the relevant mass scale in these plots is $\bar M = 2M_q/\sqrt{\lambda}$. Up to a factor of 2π, this corresponds to the mass gap in the meson spectrum (at $d=0$) [34, 35].

[12] This dimension applies in the UV where the effects of quark mass are negligible and the theory becomes conformal.

[13] Note that here we are referring to the bare or current quark mass. The constituent quark mass is certainly modified by thermal effects, as calculated in [7, 33].

[14] Ref. [11] argued that the scalars would not contribute to the condensate. In writing eq. (A.2), we have certainly ignored such scalar terms. However, strong coupling infrared dynamics might generate a condensate for the scalars. See [7] for an interesting example where the scalars dominate this expectation value at high temperatures.

[15] Note that the factor of $N_{\rm f}$ in the formulae for $\langle\tilde\psi\psi\rangle$ was overlooked in [1]. Further [11] only considers the case $N_{\rm f}=1$. A full analysis appears in [7].

JHEP02(2007)016

Now let us turn to the relation between the D7-brane gauge field and the quark-charge operator (A.1). Here the asymptotic value of the potential $A_t(\infty)$ is proportional to the coefficient with which the charge density $\mathcal{O}_{\rm q}$ enters the microscopic Lagrangian. This operator is normalized so that acting on a particular state it yields exactly the net quark density, and therefore the corresponding coefficient is precisely the chemical potential μ for the quarks. Similarly the relevant expectation value is the quark density $n_{\rm q} = \langle \mathcal{O}_{\rm q} \rangle$.

Next we provide a precise definition of the particle density on the string side of the duality. First, recall that the electric field on the worldvolume can be thought of as arising from fundamental strings 'dissolved' into the the D7-brane [20]. The density of these strings can be determined from the local charge density for the two-form B-field. The standard convention is that the fundamental string couples to the NS two-form through the worldsheet interaction $T_{\rm f} \int d^2\sigma\, B$. Hence a string pointing along the x^i-axis sources B_{ti} with the charge being just the string tension $T_{\rm f} = 1/(2\pi\ell_{\rm s}^2)$. Further, the one-form gauge invariance of B requires that the D7-brane action only involves the combination $B + 2\pi\ell_{\rm s}^2\, F$. Hence we have

$$\frac{\delta I_{\rm D7}}{\delta B_{ti}} = \frac{1}{2\pi\ell_{\rm s}^2} \frac{\delta I_{\rm D7}}{\delta F_{ti}}\,. \tag{A.3}$$

Combining these observations, we first conclude that since the D7-brane carries an electric field in the ϱ direction, the worldvolume effectively contains strings stretching along the radial direction with a density precisely determined by the electric displacement $d = -\delta I_{\rm D7}/\delta F_{t\varrho}$. The minus sign in the last expression means that for positive d the strings are oriented to be inward pointing towards the horizon at $\varrho = 1$. Since the number of strings corresponds precisely to the number of quarks in the field theory, the density of quarks is given by integrating the string density on the D7-branes over the internal three-sphere:

$$n_{\rm q} = \int d\Omega_3\, d = 2\pi^2\, d\,. \tag{A.4}$$

While d is not precisely the coefficient of the normalizable mode in eq. (2.12), the two satisfy the simple relation given in eq. (2.14).

As noted above, the non-normalizable mode $A_t(\infty)$ indicates that the charge density operator $\mathcal{O}_{\rm q}$ enters the microscopic Lagrangian. As we wish to relate this bulk mode to the chemical potential μ for the quarks in the microscopic theory, it is natural to frame the discussion in terms of the grand canonical ensemble. There the chemical potential enters the partition function as

$$\exp\left[-\beta \int d^3x\, W(\beta,\mu)\right] \equiv \sum \exp\left[-\beta \int d^3x\, \left(\mathcal{H} - \mu\, \mathcal{O}_{\rm q}\right)\right] \tag{A.5}$$

where a sum over all states is denoted on the right hand side. Of course, $W(\beta,\mu)$ and $\mathcal{H}$ are the Gibbs free energy and Hamiltonian densities, respectively. We know that $\mu \propto A_t(\infty)$ but we would like to determine the exact constant of proportionality. Towards this end, we note that, as can be seen from eq. (A.5),

$$\frac{\delta W}{\delta \mu} = -\langle\, \mathcal{O}_{\rm q}\, \rangle = -n_{\rm q}\,. \tag{A.6}$$

To compare to the string description, we turn to the semiclassical analysis of the Euclidean supergravity path integral, as described in section 3. The grand canonical ensemble is represented by the usual path integral with fixed $A_t(\infty)$ and the on-shell action gives the leading contribution to the Gibbs free energy, i.e., $I_{\rm E} = \beta W$. Hence to compare to eq. (A.6), we need to evaluate the change of the on-shell D7-brane action induced by a change of the boundary value $A_t(\infty)$. Hence given the worldvolume action (2.10), the desired variation is given by

$$\delta W = \int d\varrho\, d\Omega_3\, \delta\mathcal{L}_{\rm E} = 2\pi^2 \int_1^\infty d\varrho\, \frac{\delta\mathcal{L}_{\rm E}}{\delta\partial_\varrho A_t}\partial_\varrho \delta A_t\,, \tag{A.7}$$

where $\mathcal{L}$ is the D7-brane Lagrangian density. In eq. (A.7), we have only integrated over the internal three-sphere and the radial direction to produce the free energy density in the gauge theory directions. Once again we recognize the first factor as $d = \delta\mathcal{L}/\delta\partial_\rho A_t = -\delta\mathcal{L}_{\rm E}/\delta\partial_\rho A_t$ (in the current notation — note that we need to distinguish between the 'Lagrangian' densities appearing in the Minkowski (2.10) and Euclidean (3.1) actions), which is a constant on-shell. Hence eq. (A.7) reduces to

$$\delta W = -2\pi^2\, d\, (\delta A_t(\infty) - \delta A_t(1)) = -n_{\rm q}\, \delta A_t(\infty) \tag{A.8}$$

where we used (A.4) and the fact that A_t always vanishes on the horizon so that we must have $\delta A_t(1) = 0$. Finally comparing eqs. (A.6) and (A.8), we find

$$A_t(\infty) = \mu\,, \tag{A.9}$$

and so, as anticipated in the main text, the constant part of the asymptotic gauge potential is precisely the chemical potential for the quarks. If we wish to express results in terms of a baryon chemical potential, we would convert $\mu_{\rm b} = N_{\rm c}\,\mu$.

Let us also recall the formulae for the dimensionless quantities defined in eqs. (2.16) and (2.19) and which appear in our calculations:

$$\tilde{\mu} = \frac{2\pi\ell_{\rm s}^2\mu}{u_0} = \sqrt{\frac{2}{\lambda}}\,\frac{\mu}{T}\,, \tag{A.10}$$

$$\tilde{d} = \frac{d}{2\pi\ell_{\rm s}^2 u_0^3 N_{\rm f} T_{\rm D7}} = \frac{2^{5/2}}{N_{\rm f}N_{\rm c}\lambda^{1/2}}\,\frac{n_{\rm q}}{T^3} = \frac{2^{5/2}}{N_{\rm f}\lambda^{1/2}}\,\frac{n_{\rm b}}{T^3}\,. \tag{A.11}$$

Hence as with the previous definitions, the temperature T provides the scale to make these quantities dimensionless but implicitly we have also introduced interesting factors of the 't Hooft coupling, as well as of $N_{\rm f}$ and $N_{\rm c}$. In particular, we see that $\tilde{d}$ is naturally related to the expectation value of the baryon number $n_{\rm b}$ in (A.11).

References

[1] D. Mateos, R.C. Myers and R.M. Thomson, *Holographic phase transitions with fundamental matter*, *Phys. Rev. Lett.* **97** (2006) 091601 [hep-th/0605046].

[2] J.M. Maldacena, *The large-N limit of superconformal field theories and supergravity*, *Adv. Theor. Math. Phys.* **2** (1998) 231 [*Int. J. Theor. Phys.* **38** (1999) 1113] [hep-th/9711200].

JHEP02(2007)016

[3] O. Aharony, S.S. Gubser, J.M. Maldacena, H. Ooguri and Y. Oz, *Large-N field theories, string theory and gravity*, *Phys. Rept.* **323** (2000) 183 [hep-th/9905111].

[4] A. Karch and L. Randall, *Open and closed string interpretation of SUSY CFT's on branes with boundaries*, *JHEP* **06** (2001) 063 [hep-th/0105132];
A. Karch and E. Katz, *Adding flavor to AdS/CFT*, *JHEP* **06** (2002) 043 [hep-th/0205236].

[5] E. Witten, *Anti-de Sitter space, thermal phase transition and confinement in gauge theories*, *Adv. Theor. Math. Phys.* **2** (1998) 505 [hep-th/9803131].

[6] D. Mateos, R.C. Myers and R.M. Thomson, *Holographic viscosity of fundamental matter*, hep-th/0610184.

[7] D. Mateos, R.C. Myers and R.M. Thomson, *Thermodynamics of the brane*, hep-th/0701132.

[8] T. Albash, V. Filev, C.V. Johnson and A. Kundu, *A topology-changing phase transition and the dynamics of flavour*, hep-th/0605088;
A. Karch and A. O'Bannon, *Chiral transition of $N = 4$ super Yang-Mills with flavor on a 3-sphere*, *Phys. Rev.* **D 74** (2006) 085033 [hep-th/0605120];
T. Albash, V. Filev, C.V. Johnson and A. Kundu, *Global currents, phase transitions and chiral symmetry breaking in large-N_c gauge theory*, hep-th/0605175.

[9] O. Aharony, J. Sonnenschein and S. Yankielowicz, *A holographic model of deconfinement and chiral symmetry restoration*, hep-th/0604161;
A. Parnachev and D.A. Sahakyan, *Chiral phase transition from string theory*, *Phys. Rev. Lett.* **97** (2006) 111601 [hep-th/0604173];
Y.-h. Gao, W.-s. Xu and D.-f. Zeng, *NGN, QCD(2) and chiral phase transition from string theory*, *JHEP* **08** (2006) 018 [hep-th/0605138];
K. Peeters, J. Sonnenschein and M. Zamaklar, *Holographic melting and related properties of mesons in a quark gluon plasma*, *Phys. Rev.* **D 74** (2006) 106008 [hep-th/0606195];
E. Antonyan, J.A. Harvey and D. Kutasov, *The Gross-Neveu model from string theory*, hep-th/0608149.

[10] J. Babington, J. Erdmenger, N.J. Evans, Z. Guralnik and I. Kirsch, *Chiral symmetry breaking and pions in non-supersymmetric gauge/gravity duals*, *Phys. Rev.* **D 69** (2004) 066007 [hep-th/0306018];
I. Kirsch, *Generalizations of the AdS/CFT correspondence*, *Fortschr. Phys.* **52** (2004) 727 [hep-th/0406274].

[11] M. Kruczenski, D. Mateos, R.C. Myers and D.J. Winters, *Towards a holographic dual of large-N_c QCD*, *JHEP* **05** (2004) 041 [hep-th/0311270].

[12] A. Chamblin, R. Emparan, C.V. Johnson and R.C. Myers, *Holography, thermodynamics and fluctuations of charged AdS black holes*, *Phys. Rev.* **D 60** (1999) 104026 [hep-th/9904197];
Charged AdS black holes and catastrophic holography, *Phys. Rev.* **D 60** (1999) 064018 [hep-th/9902170].

[13] S.S. Gubser, *Thermodynamics of spinning D3-branes*, *Nucl. Phys.* **B 551** (1999) 667 [hep-th/9810225];
R.-G. Cai and K.-S. Soh, *Critical behavior in the rotating D-branes*, *Mod. Phys. Lett.* **A 14** (1999) 1895 [hep-th/9812121];
M. Cvetič and S.S. Gubser, *Phases of R-charged black holes, spinning branes and strongly coupled gauge theories*, *JHEP* **04** (1999) 024 [hep-th/9902195]; *Thermodynamic stability and phases of general spinning branes*, *JHEP* **07** (1999) 010 [hep-th/9903132].

JHEP02(2007)016

[14] R. Apreda, J. Erdmenger, N. Evans and Z. Guralnik, *Strong coupling effective Higgs potential and a first order thermal phase transition from AdS/CFT duality*, *Phys. Rev.* **D 71** (2005) 126002 [hep-th/0504151].

[15] K.-Y. Kim, S.-J. Sin and I. Zahed, *Dense hadronic matter in holographic QCD*, hep-th/0608046;
N. Horigome and Y. Tanii, *Holographic chiral phase transition with chemical potential*, hep-th/0608198;
A. Parnachev and D.A. Sahakyan, *Photoemission with chemical potential from QCD gravity dual*, hep-th/0610247.

[16] S.W. Hawking, *The path-integral approach to quantum gravity*, in *General relativity: an Einstein centenary survey*, eds. S.W. Hawking and W. Israel, Cambridge University Press, Cambridge, (1979).

[17] S.S. Gubser, I.R. Klebanov and A.W. Peet, *Entropy and temperature of black 3-branes*, *Phys. Rev.* **D 54** (1996) 3915 [hep-th/9602135].

[18] I. Racz and R.M. Wald, *Extension of space-times with Killing horizon*, *Class. and Quant. Grav.* **9** (1992) 2643.

[19] V.P. Frolov, *Merger transitions in brane-black-hole systems: criticality, scaling and self-similarity*, *Phys. Rev.* **D 74** (2006) 044006 [gr-qc/0604114];
V.P. Frolov, A.L. Larsen and M. Christensen, *Domain wall interacting with a black hole: a new example of critical phenomena*, *Phys. Rev.* **D 59** (1999) 125008 [hep-th/9811148];
M. Christensen, V.P. Frolov and A.L. Larsen, *Soap bubbles in outer space: interaction of a domain wall with a black hole*, *Phys. Rev.* **D 58** (1998) 085008 [hep-th/9803158].

[20] E. Witten, *Bound states of strings and p-branes*, *Nucl. Phys.* **B 460** (1996) 335 [hep-th/9510135].

[21] C.G. Callan Jr. and J.M. Maldacena, *Brane dynamics from the Born-Infeld action*, *Nucl. Phys.* **B 513** (1998) 198 [hep-th/9708147];
G.W. Gibbons, *Born-Infeld particles and Dirichlet p-branes*, *Nucl. Phys.* **B 514** (1998) 603 [hep-th/9709027].

[22] E. Witten, *Baryons and branes in anti de Sitter space*, *JHEP* **07** (1998) 006 [hep-th/9805112];
Y. Imamura, *Supersymmetries and BPS configurations on anti-de Sitter space*, *Nucl. Phys.* **B 537** (1999) 184 [hep-th/9807179];
C.G. Callan Jr., A. Guijosa and K.G. Savvidy, *Baryons and string creation from the fivebrane worldvolume action*, *Nucl. Phys.* **B 547** (1999) 127 [hep-th/9810092];
B. Craps, J. Gomis, D. Mateos and A. Van Proeyen, *BPS solutions of a D5-brane world volume in a D3-brane background from superalgebras*, *JHEP* **04** (1999) 004 [hep-th/9901060];
C.G. Callan Jr., A. Guijosa, K.G. Savvidy and O. Tafjord, *Baryons and flux tubes in confining gauge theories from brane actions*, *Nucl. Phys.* **B 555** (1999) 183 [hep-th/9902197].

[23] J.P. Gauntlett, C. Koehl, D. Mateos, P.K. Townsend and M. Zamaklar, *Finite energy dirac-Born-Infeld monopoles and string junctions*, *Phys. Rev.* **D 60** (1999) 045004 [hep-th/9903156].

[24] A. Hashimoto, *The shape of branes pulled by strings*, *Phys. Rev.* **D 57** (1998) 6441 [hep-th/9711097].

JHEP02(2007)016

[25] J.M. Maldacena, *Wilson loops in large-N field theories*, *Phys. Rev. Lett.* **80** (1998) 4859 [hep-th/9803002];
S.-J. Rey and J.-T. Yee, *Macroscopic strings as heavy quarks in large-N gauge theory and Anti-de Sitter supergravity*, *Eur. Phys. J.* **C 22** (2001) 379 [hep-th/9803001];
S.-J. Rey, S. Theisen and J.-T. Yee, *Wilson-Polyakov loop at finite temperature in large-N gauge theory and Anti-de Sitter supergravity*, *Nucl. Phys.* **B 527** (1998) 171 [hep-th/9803135].

[26] S.-M. Lee, A.W. Peet and L. Thorlacius, *Brane-waves and strings*, *Nucl. Phys.* **B 514** (1998) 161 [hep-th/9710097].

[27] A. Karch, A. O'Bannon and K. Skenderis, *Holographic renormalization of probe D-branes in AdS/CFT*, *JHEP* **04** (2006) 015 [hep-th/0512125].

[28] M. Henningson and K. Skenderis, *The holographic Weyl anomaly*, *JHEP* **07** (1998) 023 [hep-th/9806087]; *Holography and the Weyl anomaly*, *Fortschr. Phys.* **48** (2000) 125 [hep-th/9812032];
V. Balasubramanian and P. Kraus, *A stress tensor for Anti-de Sitter gravity*, *Commun. Math. Phys.* **208** (1999) 413 [hep-th/9902121];
R. Emparan, C.V. Johnson and R.C. Myers, *Surface terms as counterterms in the AdS/CFT correspondence*, *Phys. Rev.* **D 60** (1999) 104001 [hep-th/9903238];
C.R. Graham, *Volume and area renormalizations for conformally compact Einstein metrics*,math.DG/9909042.

[29] R.C. Myers, R.M. Thomson and A.O. Starinets, in preparation.

[30] E. Shuster and D.T. Son, *On finite-density QCD at large N_c*, *Nucl. Phys.* **B 573** (200) 434 [hep-ph/9905448]. T. Schafer and E.V. Shuryak, *Phases of QCD at high baryon density*, *Lect. Notes Phys.* **578** (2001) 203 [nucl-th/0010049].

[31] S. Nakamura, Y. Seo, S.-J. Sin and K.P. Yogendran, *A new phase at finite quark density from AdS/CFT*, hep-th/0611021.

[32] See, for example: J. Polchinski, *String theory*, vol. 2, page 163.

[33] C.P. Herzog, A. Karch, P. Kovtun, C. Kozcaz and L.G. Yaffe, *Energy loss of a heavy quark moving through $N = 4$ supersymmetric Yang-Mills plasma*, *JHEP* **07** (2006) 013 [hep-th/0605158].

[34] M. Kruczenski, D. Mateos, R.C. Myers and D.J. Winters, *Meson spectroscopy in AdS/CFT with flavour*, *JHEP* **07** (2003) 049 [hep-th/0304032].

[35] R.C. Myers and R.M. Thomson, *Holographic mesons in various dimensions*, *JHEP* **09** (2006) 066 [hep-th/0605017].

JHEP02(2007)016